



DOT/FAA/AM- 25/11

Office of Aerospace Medicine

Washington, D.C. 20591

Evaluation of Anthropomorphic Test Device Apparel for Aircraft Certification

Ian T. Hellstrom

David M. Moorcroft

William H. Carroll

Civil Aerospace Medical Institute (CAMI)

Federal Aviation Administration

Oklahoma City, OK 73169

August 2025

NOTICE

This document is disseminated under the sponsorship of the U.S. Department of Transportation in the interest of information exchange. The United States Government assumes no liability for the contents thereof.

This publication and all Office of Aerospace Medicine technical reports are available in full text from the Civil Aerospace Medical Institute's [publications website](#) and at the National Transportation Library's Repository & Open Science Access [Portal](#).



Technical Report Documentation

1. Report No. DOT/FAA/AM-25/11		2. Report Date August 2025	
3. Title & Subtitle Evaluation of Anthropomorphic Test Device Apparel for Aircraft Certification		4. Performing Organization Code AAM-632	
5. Author(s) Hellstrom, Ian T. (ORCID 0000-0002-3972-3981) Moorcroft, David M. (ORCID 0000-0002-9709-1150) Carroll, William H. (ORCID 0000-0001-6668-6971)		6. Performing Org Report Number DOT/FAA/AM-25/11	
7. Performing Organization Name & Address Civil Aerospace Medical Institute Federal Aviation Administration Oklahoma City, OK 73169		8. Contract or Grant Number N/A	
9. Sponsoring Agency Name & Address Aircraft Certification Service (AIR) Federal Aviation Administration 800 Independence Ave., S.W. Washington, DC 20591		10. Type of Report & Period Technical Report	
11. Supplementary Notes Project Sponsor: Joseph Pelletiere. Technical report DOI: https://doi.org/10.21949/1529686 The Federal Aviation Administration (FAA) funded this through the Research, Engineering, and Development (RE&D) program budget. The authors had no conflicts of interest to disclose. All authors read and approved this manuscript. This manuscript underwent an external peer review. The authors collected the data, performed the data analysis, and wrote the technical report. This document is disseminated under the sponsorship of the U.S. Department of Transportation in the interest of information exchange. The U.S. Government assumes no liability for the contents thereof.			
12. Abstract As part of a larger project aimed at gaining a better understanding of factors that affect the quality of test results using anthropomorphic test devices (ATDs), the Federal Aviation Administration (FAA) researched the effects of ATD apparel in dynamic tests. Current standards are limited to 100% cotton form fitting clothing and footwear with a 1.5-inch heel height and a combined weight of 2.5 pounds for the pair. For this project, three different types of clothing were tested: 60% cotton/40% polyester, 92% polyester/8% spandex and 100% cotton (the current standard). Additionally, four types of footwear were tested: bowling shoe, boots, sneaker, and a military specification shoe (standard). The FAA requires two certification tests to certify aircraft seating. The first test is a longitudinal impact with a minimum change in velocity of 44 ft/sec and peak acceleration of 16 g. The second test consists of a combined longitudinal-vertical impact with a minimum impact velocity of 35 ft/sec, peak acceleration of 14 g, and an impact angle of 30° off vertical. For this report, twenty-one longitudinal tests were run to measure the effects of clothing and footwear. Three additional longitudinal tests were conducted to evaluate the use of a protective barrier across the lap to mitigate damage to the ATD from the belt. Six vertical tests were conducted to evaluate the effect of the footwear in that test configuration. ATD response and seating system loads were analyzed to determine the effects of different combinations of clothing and footwear. Only minor differences were seen between the four different footwear for both longitudinal and vertical testing. The alternative clothing had little impact of peak head excursion but produced higher seat-pan loads. Thus, use of the alternate apparel could be considered a worse-case scenario. Only one of three apron tests achieved leg flail, therefore a definitive conclusion cannot be made on the impact an apron has on testing.			
13. Key Word Anthropomorphic Test Device, ATD, Certification Testing, Clothing, Footwear, Apron, Restraint, Lumbar-Spine Load, Seat-Pan Load, Floor Load, Friction, Photometrics, Aircraft Seats, Acceleration		14. Distribution Statement Document is available to the public through: National Transportation Library: https://ntl.bts.gov/ntl	
15. Security Classification (of this report) Unclassified	16. Security Classification (of this page) Unclassified	17. No. of Pages <div style="text-align: right;">70</div>	



Author Note

Funding	The research was accomplished using FAA RE&D funding programmed through the aeromedical research budget (project # A11J.FCS.28).
Conflicts of Interest	The authors had no conflicts of interest to disclose.
Author Contributions	Hellstrom: (Data Collection, Data Analysis, & Report Writing) Moorcroft: (Data Collection, Data Analysis, & Report Writing), Carroll: (Data Analysis & Report Writing)
Data Availability	Technical report DOI: https://doi.org/10.21949/1529686 , Data available at: https://doi.org/10.21949/1529691 .

Acknowledgments

The work would be unable to be completed without the support of the sponsor Joseph Pelletiere and the technical staff at CAMI, Jeff Ashmore, Ronnie Minnick, and Zachary Perkins.

Disclaimer: Mention of any product or service does not imply endorsement.



Table of Contents

Technical Report Documentation	iii
Author Note.....	iv
Acknowledgments.....	iv
List of Figures	vii
List of Tables.....	x
List of Abbreviations.....	xi
Background.....	1
Motivation.....	2
Materials and Methods.....	2
Anthropomorphic Test Device	2
Rigid Seat Fixture.....	3
Seat Pan Cushion.....	3
Restraint	4
Footwear	4
Clothing	5
Leather Apron.....	6
Test Matrix.....	7
ATD Seating Method	7
Test Pulses.....	8
Instrumentation.....	8
Video coverage	9
Coordinate-Measuring Machine.....	11
Results.....	11
Effect of Leg Flail in Longitudinal Tests.....	11
Seat and Floor Load Comparison for Full Leg Flail versus Limited Leg Flail	11
Head Path Comparison for Full Leg Flail Versus Limited Leg Flail	13
Summary – Effect of Leg Flail in Longitudinal Tests	14
Effect of Footwear	14
Longitudinal Tests	16
Vertical Tests.....	30
Summary - Effect of Footwear.....	32
Effect of Clothing in Longitudinal Tests	33
100% Cotton Comparison Tests (100% Cotton vs. 100% Cotton)	34
60% Cotton/40% Polyester vs. 100% Cotton Clothing.....	36



92% Polyester/8% Spandex vs. 100% cotton.....	41
Summary - Effect of Clothing in Longitudinal Tests.....	45
Effect of an Apron in Longitudinal Tests	46
ATD Position and Pretest Restraint Angle	47
Head Path.....	47
Seat-Pan Load	49
Floor-Pan Load	49
Seat Belt Restraint Loads	50
Pelvis Angle	51
Pelvis Damage.....	52
Summary - Effect of an Apron in Longitudinal Tests	54
Limitations.....	54
Conclusion	55
References	56
Appendix A.....	57
Appendix B	58



List of Figures

Figure 1: ATD Pelvis Damage from Lap Belt (Photo by ZIM Aircraft Cabin Solutions, LLC).	1
Figure 2: Longitudinal Test Setup: Rigid Seat and Components.	3
Figure 3: Footwear Tread Patterns (Left to Right): Mil Spec, Boots, Bowling Shoe, and Sneakers.....	5
Figure 4: Tested Clothing (Left to Right): 100% Cotton, 60% Cotton/40% Polyester, and 92% Polyester/8% Spandex.....	5
Figure 5: ATD with Leather Apron Seated for Longitudinal Test.....	6
Figure 6: Longitudinal and Vertical Achieved Pulses.....	8
Figure 7: ATD Instrumentation Coordinate System SAE J1733 (SAE International, 2024).	9
Figure 8: Overhead View of Camera Layout.	10
Figure 9: Resultant Seat-Pan and Floor-Pan Loads for A22003 (Flail) and A22006 (Limited Flail).....	12
Figure 10: ATD Position at 110 (Left), 160 (Center) and 220 ms (Right), A22003.	12
Figure 11: ATD Position at 110 (Left), 160 (Center) and 200 ms (Right), A22006.	12
Figure 12: Head Path for Full Flail and Limited Flail.	13
Figure 13: Example of Full Head Excursion in X-Direction (Left) and Minimum Z-Position (Right).	14
Figure 14: Bent Knee Bracket at Completion of A21015.	15
Figure 15: Head Path for Baseline: X-position vs Z-Position.	17
Figure 16: Head Path for Baseline: X and Z-Position vs. Time.	18
Figure 17: Floor Load in X-Direction for Baseline.	18
Figure 18: Head Path for Boots and Mil Spec: X-position vs Z-Position.	20
Figure 19: Head Path for Boots and Mil Spec: X-Position vs Time.	20
Figure 20: Head Path for Boots and Mil Spec: Z-Position vs Time.	21
Figure 21: Floor-Pan Loads in X-Direction (Boots vs Mil Spec).	22
Figure 22: A21011 (Boots) Peak Load Floor-Pan Load at 52 ms (Left) and Last Frame at 119 ms (Right).	22
Figure 23: A22002 (Boots) Peak Load Floor-Pan Load at 62 ms (Left) and Last Frame at 130 ms (Right).	22
Figure 24: A22009 (Mil Spec) Peak Load Floor-Pan Load at 64 ms (Left) and Last Frame at 154 ms (Right).	23
Figure 25: Head Path for Bowling Shoe and Mil Spec: X-Position vs. Z-Position.....	24
Figure 26: Head Path for Bowling Shoe and Mil Spec: X-Position vs. Time.....	24
Figure 27: Head Path for Bowling Shoe and Mil Spec: Z-Position vs. Time.....	25
Figure 28: Floor Load in X-Direction (Bowling Shoe and Mil Spec).	26
Figure 29: A22001 Peak Load Floor Load at 51 ms (Left) and Last Frame at 115 ms (Right). ..	26



Figure 30: Head Path for Sneakers and Mil Spec: X-Position vs Z-Position.	27
Figure 31: Head Path for Sneakers and Mil Spec: X-Position vs. Time.	28
Figure 32: Head Path for Sneakers and Mil Spec: Z-Position vs. Time.	28
Figure 33: Floor-Pan Loads in the X-Direction (Sneakers and Mil Spec).	29
Figure 34: Photo of Peak Load in A22011 (Sneakers) at 75 ms (Left) and Last Photo with Feet on Floor at 141 ms (Right).	29
Figure 35: Leg Angle Dimension for the Vertical Tests and CMM Coordinate System.	30
Figure 36: Lumbar Loads in Z-Direction for Vertical Tests.	31
Figure 37: Seat-Pan Load in Z-Direction for Vertical Tests.	32
Figure 38: Floor-Pan Load in Z-Direction for Vertical Tests.	32
Figure 39: Footwear Head Excursion Average and Range Bar Chart.	33
Figure 40: Seat-Pan Force in the X-Direction (Baseline).	35
Figure 41: Belt-Transducer Loads for Baseline.	35
Figure 42: Change in Pelvis Angle about Y-Axis for Baseline.	36
Figure 43: Head Path for 60/40 and Cotton: X-Position vs. Z-Position.	37
Figure 44: Head Path for 60/40 and Cotton: X-Position vs. Time.	38
Figure 45: Head Path for 60/40 and Baseline: Z-Position vs. Time.	38
Figure 46: Seat-Pan Force in the X-Direction (60/40 and Cotton).	39
Figure 47: Belt-Transducer Loads (60/40 and Cotton).	40
Figure 48: Change in Pelvis Angle about Y (60/40 and Cotton).	40
Figure 49: Head Path for 92/8 and Cotton: X-Position vs. Z-Position.	42
Figure 50: Head Path for 92/8 and Cotton: X-Position vs. Time.	42
Figure 51: Head Path for 92/8 and Cotton: Z-Position vs. Time.	43
Figure 52: Seat-Pan Loads in the X-Direction (92/8 and Cotton).	43
Figure 53: Seat Belt Loads (92/8 and Cotton).	44
Figure 54: Change in Pelvis Angle about Y (92/8 and Cotton).	45
Figure 55: Clothing Head Path Bar Chart.	46
Figure 56: Head Path for Baseline and Apron.	48
Figure 57: Head Path for Apron and Baseline: X & Z-Position vs. Time.	48
Figure 58: Seat-Pan Load in X-Direction for Apron and Baseline.	49
Figure 59: Floor Load in X-Direction for Apron and Baseline.	50
Figure 60: A22008 Picture of Peak Floor Load at 137 ms (Left) and Last Frame with Feet Touching Floor Pan at 158 ms (Right).	50
Figure 61: Belt-Transducer Load for Apron and Baseline.	51
Figure 62: Change in Pelvis Angle about Y (Apron and Baseline).	52
Figure 63: ATD Pelvis Damage from Belt Buckle after Seven Longitudinal Tests.	52
Figure 64: Damage to Pelvis at Completion of Testing.	53

Figure 65: Leather Apron Damage After One Test.	53
Figure 66: Leather Apron Damage at the Completion of testing. Permanent Marker for Position and Scale of Hole.....	54



List of Tables

Table 1: Footwear Specifications.	4
Table 2: Testing Matrix.....	7
Table 3: Instrumentation List.	9
Table 4: Tests Discussed in the Effect of Leg Flail.	11
Table 5: Head Path Values for Full Flail and Limited Flail.	13
Table 6: Initial Ankle Position.	15
Table 7: Tests Discussed in the Effect of Footwear.....	16
Table 8: Head Path Values (Baseline).	17
Table 9: Head Path Values (Boots and Mil Spec).....	19
Table 10: Head Path Values (Bowling and Mil Spec).	23
Table 11: Head Path Values (Sneakers and Mil Spec).....	27
Table 12: Peak Load Cell Value for Lumbar, Seat-Pan and Floor Load.	31
Table 13: Tests Discussed in the Effect of Clothing.....	34
Table 14: Head Path Values (60/40 and Cotton).	37
Table 15: Seat-Pan Loads (60/40 and Cotton).	39
Table 16: Head Path Values (92/8 and Cotton).	41
Table 17: Seat-Pan Loads (92/8 and Cotton).	44
Table 18: H-Point Pretest Position Values.....	47
Table 19: Pretest Belt Angles.....	47
Table 20: Seat-Pan Loads (Apron and Baseline).	49
Table 21: Peak Seat Belt Loads (Apron and Baseline).....	51
Table 22: Mil Spec Coefficient of Friction Measurements and Calculation (Average=0.97).	57
Table 23: Boots Coefficient of Friction Measurements and Calculation (Average=1.00).....	57
Table 24: Bowling Shoe Coefficient of Friction Measurements and Calculation (Average=0.62).	57
Table 25: Sneaker Coefficient of Friction Measurements and Calculation (Average=1.32).....	57



List of Abbreviations

2-D	two dimensional
60%/40% poly or 60/40	60% cotton/40% polyester
92%/8% poly or 92/8	92% polyester & 8% spandex
AWS	Amazon Web Service
DMP	Data Management Plan
deg/sec	angular velocity
ATD	Anthropomorphic Test Device
CG	center of gravity
CAMI	Civil Aerospace Medical Institute
CFR	Code of Federal Regulations
cm	centimeter
CMM	Coordinate Measuring Machine
deg or °	degree
DOE	Design of Experiments
DOI	Digital Object Identifier
DOT	Department of Transportation
FAA	Federal Aviation Administration
ft./sec	feet per second
g	gravity
H-point	hip joint center point
in.	inch
kg	kilogram
lb.	pounds (force)
mil spec	Military Specification Dress Shoe
mm	millimeter
ms	millisecond
SRP	Seat Reference Point
S&G	Sprague and Geer's



Background

The Federal Aviation Administration (FAA) has regulations in place that require aircraft seating systems protect occupants in the event of an emergency landing (Emergency Landing Dynamic Conditions, 14 C.F.R. §25.562, 2022). Dynamic testing using Anthropomorphic Test Devices (ATDs) is required by these regulations to substantiate the safety of seating systems. Two certification tests are specified, one consists of a longitudinal impact with a minimum change in velocity of 44 ft/sec and peak acceleration of 16 g and the second consists of a combined longitudinal-vertical impact with a minimum impact velocity of 35 ft/sec, peak acceleration of 14 g, and an impact angle of 30° off vertical. How the ATD interacts with the seat and simulated aircraft floor affects the overall system response, with the ATD's clothing and footwear potentially playing a significant role. SAE International Aerospace Standard 8049D (AS8049D) specifies the ATD clothing and footwear for dynamic testing in section 5.3.2.1 (SAE International, 2020). "Each ATD should be clothed in form-fitting cotton stretch garments with short to full length sleeves, mid-calf to full length pants and size 11E (45) shoes weighing about 2.5 pounds (1.1 kg) and having a heel height of about 1.5 in. (3.8 cm)." The seat testing industry has noted challenges in obtaining compliant clothing.

The harsh nature of dynamic testing results in damage to the ATD. It is common for the rubber and foam cover to develop cuts and punctures from seat belt interaction. *Figure 1*, from ZIM Aircraft Cabin Solutions, LLC, illustrates such damage. Due to the cost and time associated with replacing damaged parts, the FAA has been asked by industry if a protective barrier, such as a leather apron, could be placed between the ATD and the lap belt. While a reinforcement barrier may mitigate damage to the rubber and foam cover, it could also adversely affect the ATDs kinematics.

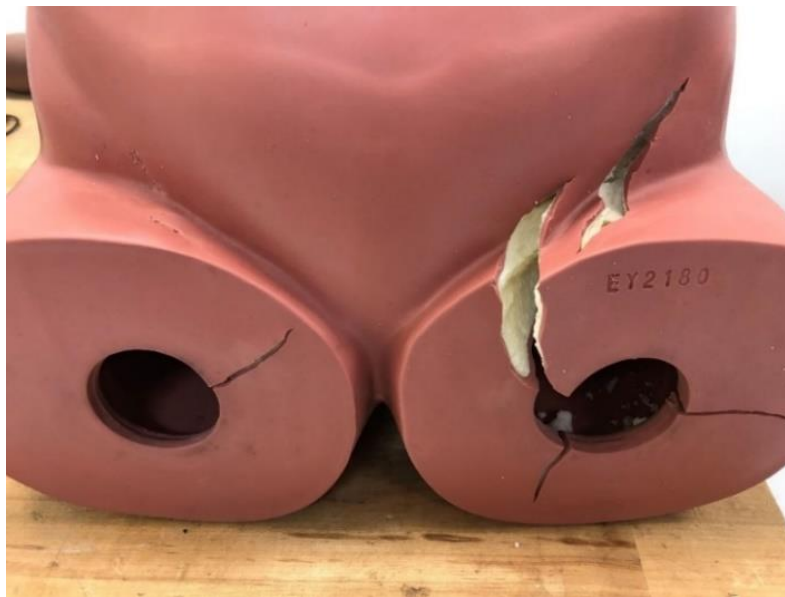


Figure 1: ATD Pelvis Damage from Lap Belt (Photo by ZIM Aircraft Cabin Solutions, LLC).

Motivation

The Policy and Standards Division (AIR-600) needs to identify the data variability attributable to ATDs and their apparel during aircraft seat certification. This research seeks to establish standardized clothing requirements for future certification testing. To fulfill this requirement, various apparel combinations were tested in both longitudinal and combined longitudinal-vertical impact tests. Longitudinal testing assessed changes in kinematics due to footwear, clothing, and the addition of a leather apron. Combined longitudinal-vertical testing will be used to assess the effect of footwear on ATD response.

Materials and Methods

This research protocol consisted of testing and analyzing combinations of clothing and footwear. The three types of clothing varied in coefficients of friction, while the footwear differed in coefficients of friction at the sole, weight, and heel height. The tests were designed to analyze the variance in the sensor data and video derived data across these combinations. Non-standard clothing and footwear were compared to baseline items that met AS8049D specifications (clothing of 100% cotton and footwear of 2.5 lb. weight with 1.5 in. heel height). Additionally, a leather apron was tested as a protective barrier to determine its potential to inhibit the movement of the ATD. The clothing, footwear, and apron combinations were evaluated in a longitudinal impact. In the combined longitudinal-vertical (hereafter referred to as vertical) tests, the footwear was evaluated for compression and change in ATD response. The apron was not evaluated in the vertical testing because the load path of the ATD during a downward impact is directed into the seat pan rather than through the seatbelt; therefore, the apron, which interfaces primarily with the belt, is not loaded in these conditions.

Anthropomorphic Test Device

The 50th percentile FAA Hybrid III ATD was used to assess injury risk. This ATD is a modification of the automotive Hybrid III, incorporating parts of the Hybrid II to make it acceptable for aviation testing (Gowdy et al., 1999). Figure 2 shows the FAA Hybrid III ATD in a longitudinal test configuration. The pelvis, manufactured in June of 2016, had no visible external damage at the start of testing.



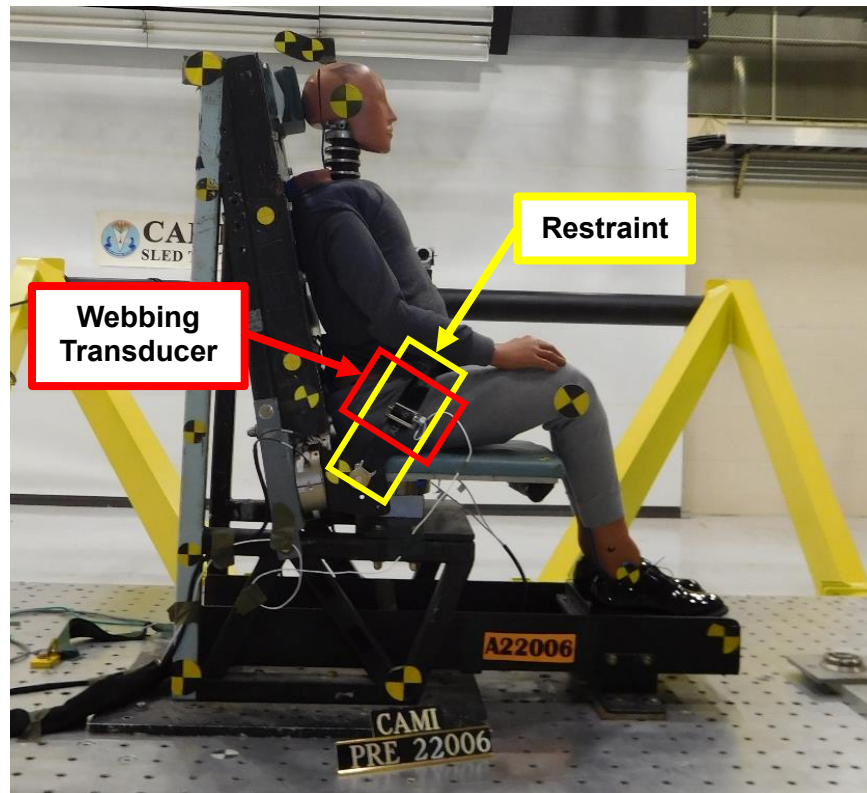


Figure 2: Longitudinal Test Setup: Rigid Seat and Components.

Rigid Seat Fixture

The longitudinal and vertical tests used a rigid seat frame comprised of welded 2-in. square steel tubing ([Figure 2](#)). The seat back consisted of an aluminum plate with a recline angle of 12.5°. Four load cells were mounted to the frame to collect load data from the seat pan, floor, and the two restraint anchor points. Aluminum plates were used for the seat pan and floor pan, and each plate was mounted directly to a load cell and parallel to the sled floor. A carpet covered the floor pan to produce a realistic interaction between the floor and the footwear. The floor pan height was set to achieve 13 in. between the ATD's hip joint center point (H-point) and the center of the ankle pivot.

Seat Pan Cushion

A 1-in. thick green Confor™ seat cushion with a leather cover was mounted to the seat pan using hook and loop tape. The thin cushion combined with a leather cover was selected to maximize ATD movement. Different cushion and cover configurations, such as a cloth cover and thick contoured cushion, could have inhibited the ATDs movement compared to the combination selected for testing. The cushion placement is shown in [Figure 2](#).

Restraint

A standard 2-point pelvic restraint made of polyester webbing was used during testing. Restraint mounting points were located following AS8049D §3.2.15 which states, "...the pelvic restraint system shall be designed such that the vertical angle between the pelvic restraint centerline and the SRP [seat reference point] waterline shall range from 35 to 55 degrees...the pelvic restraint anchorage point(s) must be located no further than 2.0 in. (51 mm) forward of the SRP" (SAE International, 2020). The angles achieved in testing ranged from 40.6° to 49.3° with an average angle of 42.2°. [Figure 2](#) shows the nominal belt placement for this project. A new restraint was used every test due to ATD free flail generating high restraint webbing loads during longitudinal tests. The webbing on the shorter side of the restraint was 12 in. long. After the restraint was tightened during the pretest set up, the buckle was not centered on the ATD. To mitigate damage accruing on only one side of the pelvis, the side the buckle was mounted to was switched between sides throughout testing. A webbing transducer was used to collect load data, and this transducer was installed on the ATD's right side for every test, as shown in [Figure 2](#).

Footwear

The types of footwear tested included Timberland PRO Titan Soft Toe hiking boots (boots), Bates High Gloss Oxford military specification dress shoe (mil spec), Dexter Dex Lite Pro bowling shoe, and Skechers Flex sneakers. All footwear was obtained through Amazon.com. [Table 1](#) has heel heights and weights for the footwear tested. The footwear used in this series had a heel height ranging from 1.25 in. to 1.85 in. When acquiring the footwear, effort was made to match the AS8049D requirements of 1.5 in., but compromises were made to achieve a variety of tread types. The bowling shoe and sneakers were lighter than the specification, the mil spec was the closest to the 2.5 pounds (lb.), and the boots were heavier at approximately 3 lb.

Table 1: Footwear Specifications.

	8049D Specification	Mil Spec	Boots	Bowling Shoe	Sneakers
Average Heel Height (in.)	1.50	1.44	1.85	1.25	1.28
Average Weight per Shoe (lb.)	1.25	1.22	1.55	0.84	0.77

Prior to the dynamic sled tests, the dynamic friction coefficients were calculated by sliding the footwear across carpet with various weights and recording the force with a push gauge. Three separate weights were placed in the footwear and then drug over the same carpet used on the rigid seat. The coefficient of friction was calculated by dividing the measured sliding force by the weight of the footwear plus the weight inside. [Appendix A](#) contains the data gathered from these tests. The four measurements were averaged, producing the following coefficients of dynamic friction: 1.32 (sneakers), 1.00 (boots), 0.97 (mil spec), and 0.62 (bowling shoe). The tread patterns of the footwear are shown in [Figure 3](#). In the vertical tests, the boots (hardest sole material) and the sneakers (softest sole material) were selected to evaluate any change in ATD response.



Figure 3: Footwear Tread Patterns (Left to Right): Mil Spec, Boots, Bowling Shoe, and Sneakers.

Clothing

A 100% cotton set consisting of a long sleeve shirt and full-length pants served as the baseline clothing set. This set was made by Therma Tek with a material thickness of 0.07 inches and weighed 0.81 lb. Two additional clothing sets were tested: 60% cotton/40% polyester (abbreviated 60%/40% poly or 60/40), manufactured by Place & Street with a thickness of 0.07 inches and a weight of 0.79 lb., and 92% polyester/8% spandex (abbreviated 92%/8% Poly or 92/8), produced by Weerti with a thickness of 0.06 inches and weighing 0.95 lb. All clothing was obtained through Amazon.com and met the criteria for form fitting, long sleeve shirt, and full-length pants. [Figure 4](#) shows pretest photos of the different clothing tested.



Figure 4: Tested Clothing (Left to Right): 100% Cotton, 60% Cotton/40% Polyester, and 92% Polyester/8% Spandex.

The clothing coefficient of friction was determined using the clothing, the cushion cover, and an ATD pelvis. The pelvis was placed on top of the clothing, then the clothing was pulled across the leather cover with a push-pull gauge to measure the force. The coefficient of friction was calculated by dividing the sliding force by the weight of the pelvis. The coefficient of dynamic friction values for the clothing were: 0.23 for 100% cotton, 0.27 for 60% cotton/40% polyester, 0.29 for 92% polyester/8% spandex.

Leather Apron

Three longitudinal tests were conducted using a 3/16 in. thick leather apron placed between the ATD and the seat belt. The leather apron measured 20 in. by 15 in. and included relief cuts to aid in the formfitting of the apron across the ATD's lap. [Figure 5](#) shows how the apron was placed on the ATD during test setup. The leather apron was tested with the baseline clothing combination: 100% cotton clothing and mil spec footwear. The leather apron tests evaluated both static and dynamic differences. The static evaluation checked both the pretest belt angles and ATD positioning. The dynamic tests evaluated any changes to ATD movement, load data, and damage mitigation to the ATD components.

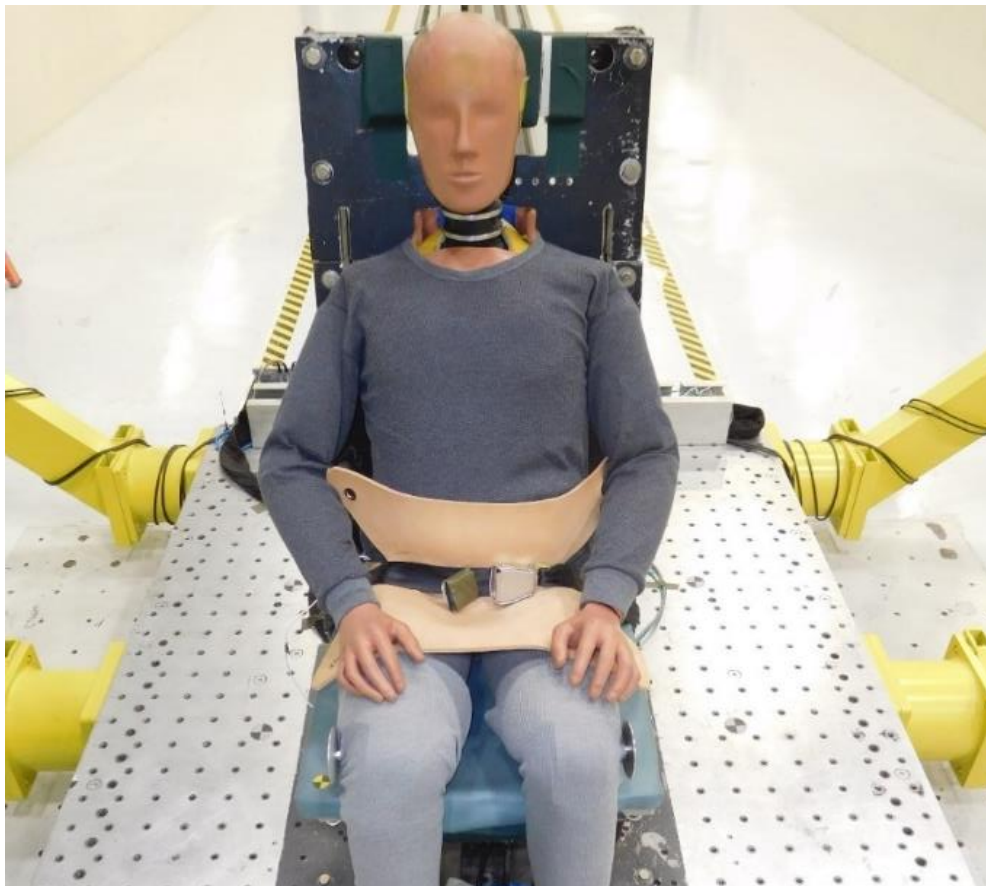


Figure 5: ATD with Leather Apron Seated for Longitudinal Test.

Test Matrix

Table 2: Testing Matrix. provides the test matrix for the 30 tests conducted. It outlines the variables of clothing, footwear, seat orientation, and the number of tests run. A Design of Experiments (DOE) approach to test planning was used to develop the test matrix. Two variables used as the input to the DOE: clothing friction and footwear friction. The two variables created four extremes:

- high friction clothing-high friction footwear (test series 1)
- high friction clothing-low friction footwear (test series 2)
- low friction clothing-high friction footwear (test series 4)
- low fiction clothing-low friction footwear (test series 5)

Both test series 3 and 6 were combinations of clothing and footwear selected at random. Test series 7 used the AS8049D defined apparel. Test series 8 used the AS8049D apparel with the addition of the leather apron. Test series 9 and 10 were the vertical tests with the hardest (test series 9) and softest (test series 10) sole material. Most test series, three tests were performed.

Table 2: Testing Matrix.

Test Series	Seat Orientation	Clothing	Footwear	Number of Tests
1	Longitudinal	92%/8% Poly	Sneakers	3
2	Longitudinal	92%/8% Poly	Bowling	3
3	Longitudinal	60%/40% Poly	Sneakers	2
4	Longitudinal	100% Cotton	Sneakers	3
5	Longitudinal	100% Cotton	Bowling	4
6	Longitudinal	100% Cotton	Boots	3
7	Longitudinal	100% Cotton	Mil Spec	3
8	Longitudinal	100% Cotton & Apron	Mil Spec	3
9	Vertical	100% Cotton	Boots	3
10	Vertical	100% Cotton	Sneakers	3

ATD Seating Method

The ATD was seated following the guidance in AS8049D which involves lowering the ATD into the seat while holding the thighs horizontal, then pushing the ATD rearward with approximately 20 lb. of force. This method produces a consistent fore/aft position and initial pelvis angle (Moorcroft et al., 2010). Markers were placed on the ATD pelvis at the projection of the H-point, an auxiliary target directly above that point (vertical H-point target), and at the head center of gravity (CG). A three-dimensional coordinate measuring machine (CMM) was used to record the ATD head center of gravity photometric target, as well as the H-point and vertical pelvis targets.

These measurements were used to derive the pelvic angle (based on the H-point and vertical H-point) and torso angle (based on a line between the head CG and H-point). The average location of the ATD H-point, vertical H-point and head CG from the longitudinal tests was used to define the goals for the vertical seating. Cloth-covered, closed-cell foam shims were used during the

vertical testing to position the ATD in the same fore/aft position and angle relative to when seated horizontally.

Test Pulses

Two dynamic test conditions were evaluated: longitudinal tests at 16 g and vertical tests at 14 g. These test pulses correspond with those specified in 14 CFR §25.562. The longitudinal tests used an isosceles triangle-shaped impact pulse with an acceleration of 16 g and a minimum velocity change of 44 ft/sec. The vertical tests used an isosceles triangle shaped impact pulse with an acceleration of 14 g and a minimum velocity change of 35 ft/sec, with an impact angle of 30 degrees from vertical. Examples of achieved pulses for the longitudinal and vertical testing are provided in [Figure 6](#).

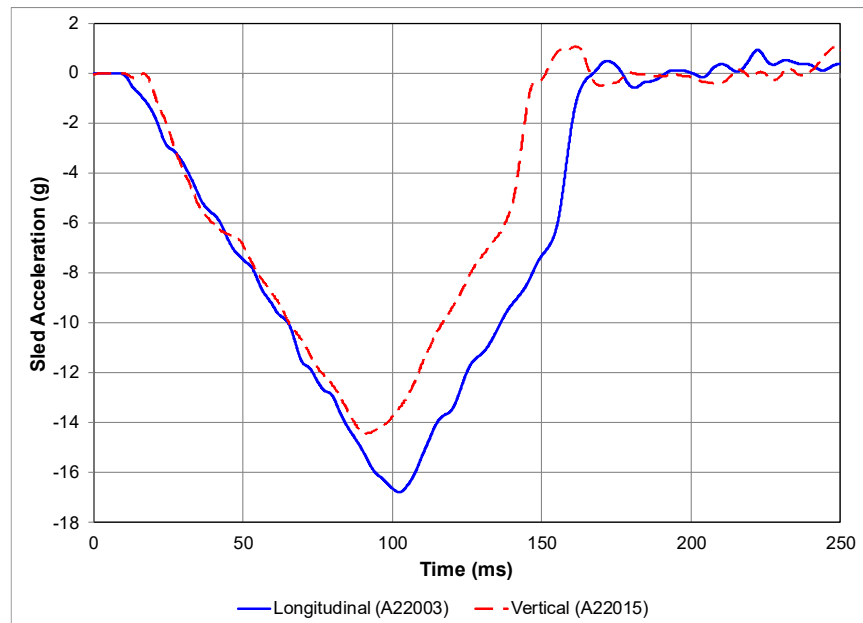


Figure 6: Longitudinal and Vertical Achieved Pulses.

Instrumentation

Electronic instrumentation included sensors on the sled, ATD, and rigid seat as outlined in [Table 3](#). For this project, load cells were mounted on the seat pan, floor pan, and seat pan anchor points to measure the loads generated by the ATD into the rigid seat. The test data was gathered and filtered per the requirements of SAE J211-1 (SAE International, 2022a). The sign convention of the recorded signals conformed to SAE J1733 (SAE International, 2024) (see [Figure 7](#)). Load cell data were tare corrected to eliminate the inertial effect of the fixture and internal load cell mass.

Table 3: Instrumentation List.

Description	Units	Filter Class
Sled Acceleration	g	60
Seat-Pan Force (F_x , F_y , F_z)	lb.	60
Floor-Pan Force (F_x , F_y , F_z)	lb.	60
Belt Anchor Force (F_x , F_y , F_z)	lb.	60
Belt Webbing Transducer	lb.	60
Head Acceleration (A_x , A_y , A_z)	g	1000
Upper Neck Force (F_x , F_y , F_z)	lb.	1000
Upper Neck Moments (M_x , M_y , M_z)	in.-lb.	600
Lumbar Force (F_x , F_y , F_z)	lb.	600
Lumbar Moment (M_x , M_y , M_z)	in.-lb.	600
Pelvis Acceleration (A_x , A_y , A_z)	g	1000
Pelvis Angular Velocity (R_x , R_y , R_z)	deg/sec	180

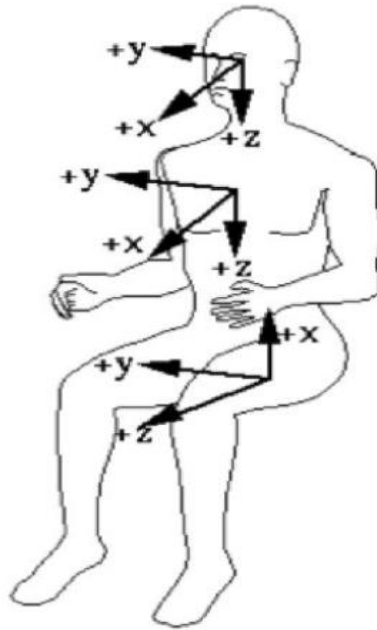


Figure 7: ATD Instrumentation Coordinate System SAE J1733 (SAE International, 2024).

Video coverage

High-speed color video was captured using onboard cameras recording at 1,000 frames per second with a resolution of 2016 x 2016 pixels. Four cameras were mounted perpendicular to the direction of the sled, two on each side (see Figure 8). Targets were placed on the head center of gravity, a rigid plate on the knee joint, a rigid plate on the ankle joint, and two auxiliary targets mounted above the head. Pelvis H-point targets were omitted to maximize contact between the

seat belt and the clothing¹. Targets were placed on rigid structures for scaling, validation, and subtracting relative motion between the sled and the camera.

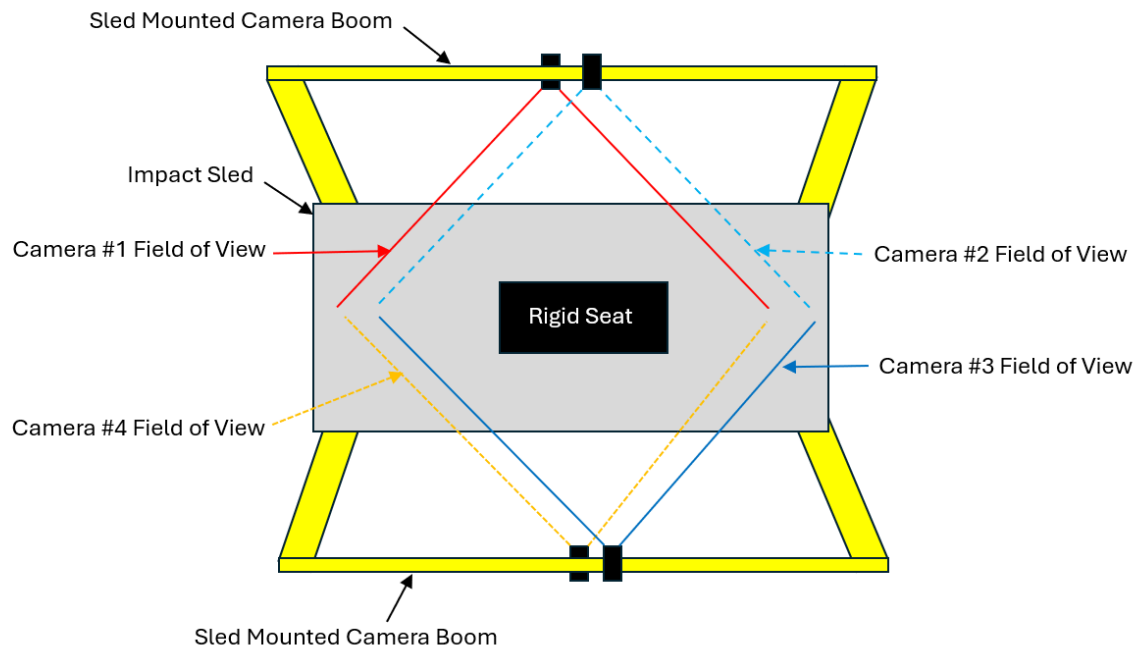


Figure 8: Overhead View of Camera Layout.

The position of targeted points was derived from the videos using procedures specified in SAE J211/2 (SAE International, 2022b). The photometric data analysis positive X-direction is the same direction as the instrumentation positive (as defined in J1733). However, the positive Z-direction in the photometric analysis is up, which is the opposite of J1733.

The head path was determined by collecting the 2-D coordinates from each frame and applying a spline-fit to construct a smooth curve throughout the video. The two auxiliary targets on the head were used to facilitate tracking of the head CG when the arms obscured a direct view. Experience has shown that obscuration typically occurs at or near the peak forward motion of the head. Since the auxiliary targets were rigidly mounted to the head, the position of the head can be determined using a virtual point and geometry.

¹ In certification tests, the pants may be cut to facilitate view of the H-point target. "The ATD clothing shall be removed locally where targets are attached to the ATD. Sufficient clothing shall be removed around the target to prevent obstruction of the target during the test." [AS8049D 5.3.4.2.a].

Coordinate-Measuring Machine

A coordinate-measuring machine (CMM) was used to collect pretest setup position data for multiple points on the ATD, monuments on the sled/seat structure, and the seat belt restraint. The CMM coordinate system used the same positive directions as the system used in photometric analysis.

Results

Effect of Leg Flail in Longitudinal Tests

AS8049D states, “Floors should not influence the behavior of the seat or unduly restrict the movement of the ATD’s feet...” Two tests were compared to determine the effect of leg flail on occupant response ([Table 4](#)). In test A22003, full leg flail was achieved, whereas test A22006 only achieved flail with the right leg.

Table 4: Tests Discussed in the Effect of Leg Flail.

Test	Clothing	Footwear	Flail
A22003	100% Cotton	Mil Spec	Full
A22006	100% Cotton	Mil Spec	Limited

Seat and Floor Load Comparison for Full Leg Flail versus Limited Leg Flail

Two tests that utilized the AS8049D clothing and footwear combination were selected to illustrate the difference in results for a test where the legs fully flailed (A22003) and a test where only one leg flailed (A22006). Test A22003 both feet slide off the floor at about 110 milliseconds (ms) and in A22006 the right leg slides off at the same time. Both tests had similar ATD motion of the torso throughout. Nominally, these two tests were identical, using the same apparel and same initial position (most importantly, the same X-position of the ankles and angle of the lower leg).

[Figure 9](#) has the plots of the resultant seat-pan and floor-pan loads for both tests. For the full leg flail test (A22003), the resultant floor load peaks around 200 lb., while it exceeds 2000 lb. in the limited flail test (A22006). Much of the floor load in A22006 is in the Z-direction. When there is limited flail, the load generated by the ATD in the Z-direction is distributed between the floor pan and seat pan. As a result, the seat-pan resultant loads also diverge in these two tests, with the full flail test producing about three times the seat-pan load as the limited flail test. These results show that the seat is not fully loaded by the ATD when the legs do not fully flail. From 0-110 ms, the loads and kinematics are the same; the loads only differ beyond 110 ms. For full flail, both thighs push the seat pan aft, while in the partial flail case, only one thigh does (while the other thigh loads the floor). The spike after 200 ms due to the chest impacting the thighs.

[Figure 10](#) (A22003) and [Figure 11](#) (A22006) show the different ATD positions at the three local seat-pan peaks. The first and second seat-pan load peaks were achieved at 110 ms and 160 ms respectively. The third peak in both tests occurred when there was chest to thigh contacts.

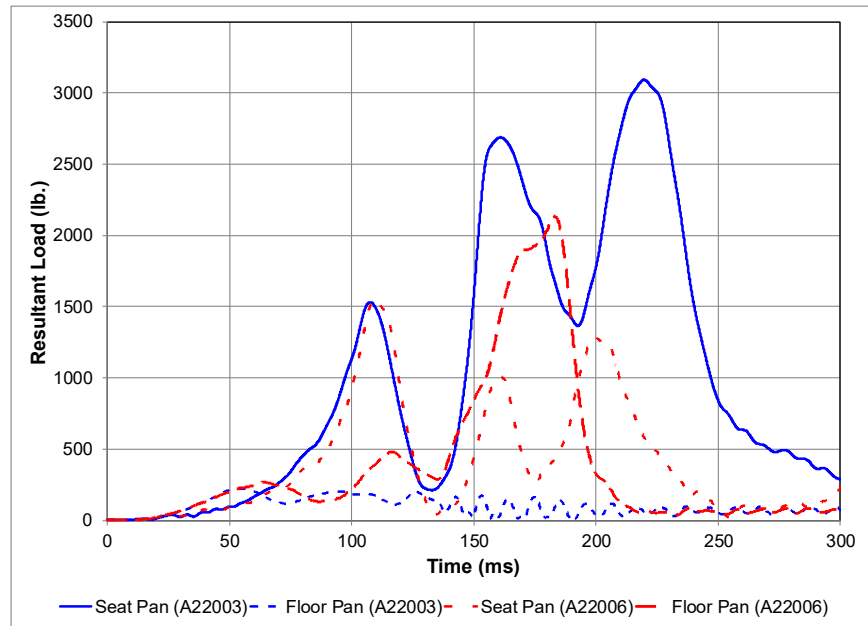


Figure 9: Resultant Seat-Pan and Floor-Pan Loads for A22003 (Flail) and A22006 (Limited Flail).



Figure 10: ATD Position at 110 (Left), 160 (Center) and 220 ms (Right), A22003.



Figure 11: ATD Position at 110 (Left), 160 (Center) and 200 ms (Right), A22006.

Head Path Comparison for Full Leg Flail Versus Limited Leg Flail

The initial positions and maximum values for the head path, based on the head CG target, for the two comparison tests are presented in [Table 5](#). The limited-flail test's maximum X-position was 2.4 in. less and 8.2 in. less in Z-position compared to the full-flail test. Limited leg flail also affected the ATD's motion throughout the dynamic test ([Figure 12](#)). [Figure 13](#) shows still frames from test A22003 to show head position at full excursion for the X-direction and the minimum Z-position.

Table 5: Head Path Values for Full Flail and Limited Flail.

Test	Clothing	Footwear	X-Position at t=0 (in.)	Z-Position at t=0 (in.)	Max X-Position (in.)	Time (ms)	Min Z-Position (in.)	Time (ms)
A22003	100% Cotton	Mil Spec	5.8	45.2	44.5	175	6.0	222
A22006	100% Cotton	Mil Spec	5.2	45.2	42.1	168	14.2	205

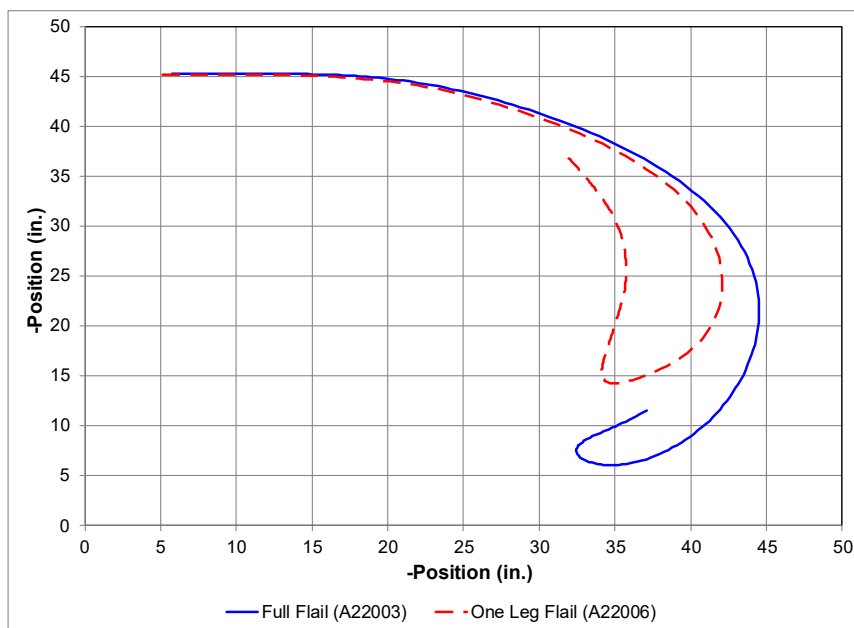


Figure 12: Head Path for Full Flail and Limited Flail.

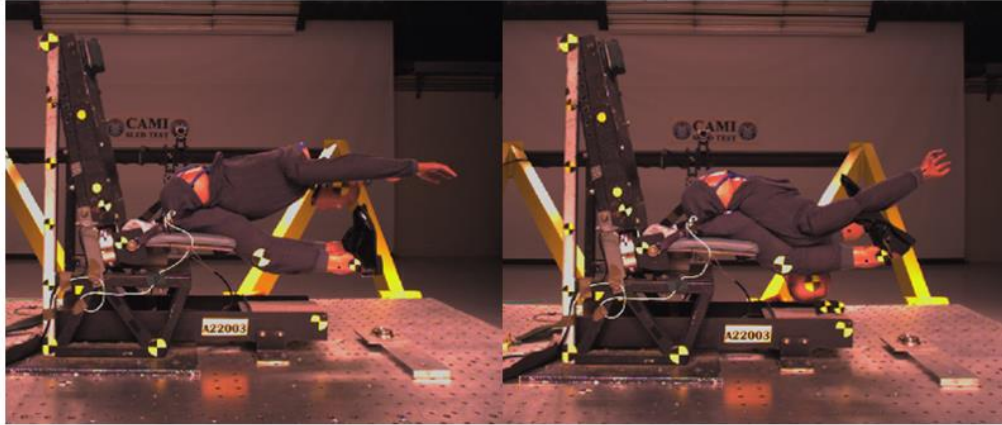


Figure 13: Example of Full Head Excursion in X-Direction (Left) and Minimum Z-Position (Right).

Summary – Effect of Leg Flail in Longitudinal Tests

Longitudinal tests conducted according to AS8049D require unrestricted leg flail to allow for maximum loading of the seat structure. This test series demonstrated that when the legs do not flail, the floor-pan load increases and the seat-pan load decreases by as much as 1800 lb., resulting in the aircraft seat not being fully loaded through its primary load paths. Additionally, the occupant motion was affected in the limited flail scenarios (e.g. change in head path by 2.5 in.), therefore, all limited flail tests were excluded from the comparisons in this report.

Effect of Footwear

Since the presence or absence of leg flail strongly influences ATD response, all the longitudinal tests were assessed for leg flail. Sixteen tests had full leg flail, and eight tests had limited leg flail (i.e., at least one leg remaining in contact with the floor). All tests using boots or bowling shoe produced full leg flail. Three mil spec tests had one leg that did not flail; two of these three tests were with the apron. The sneakers limited leg flail in five of the eight tests. In the first three tests with the sneakers, A21007, A21010, and A21015, neither leg flailed. To encourage flail in test A21016 the sneakers were placed 1 in. forward of the heel stop. One leg flailed in test A21016. The feet were moved forward of the heel stop by 2 in. for tests A22005, A22011, A22012, and A22013. Of these four, only test A22013 did not achieve full leg flail.

Lack of leg flail creates another undesirable loading condition within the ATD. In Test A21015 the right leg did not flail, transmitting load through the floor pan-enough to bend the knee bracket. The force was high enough to bend the knee bracket and render it unsuitable for further testing. The bracket was replaced prior to subsequent tests.



Figure 14: Bent Knee Bracket at Completion of A21015.

Ankle position was recorded prior to every test. Table 6 summarizes the range of ankle position values, the average position, and the flail results. For the mil spec, there was no significant difference in the range of ankle position between the tests where the leg flailed vs when the leg did not flail. In contrast, the sneakers, the ankles had to be moved 2 in. forward to induce leg flail.

As noted previously, there was a range of dynamic friction coefficients: 1.32 (sneakers), 1.00 (boots), 0.97 (mil spec), and 0.62 (bowling shoe). Based on these values, it makes sense that the bowling shoe tests would all exhibit flail and the sneakers would require additional effort to ensure flail. The boots, despite having a slightly higher coefficient than the mil spec, did not have any foot stick issues. This may be due to the additional ankle support and the ankle target contacting the top edge of the boot, which likely dampened ankle rotation and reduced the duration the sole was in contact with the carpet. In contrast, the mil spec occasionally exhibited foot sticking. Thus, the presence, or absence, of leg flail was dependent on the type of shoe for the ankle positions tested. Other leg positions, particularly pure vertical or with the ankle behind the knee, could result in a more pronounced effect.

Table 6: Initial Ankle Position.

Shoe	Flail	Minimum X-Position of Ankle (in.)	Maximum X-Position of Ankle (in.)	Average X-Position (in.)
Mil Spec	Yes	25.2	25.9	25.5
Mil Spec	No	25.3	25.6	25.5
Sneakers	Yes	27.2	27.6	27.3
Sneakers	No	25.0	27.0	25.9
Boots	Yes	25.2	25.6	25.3
Bowling	Yes	25.2	25.4	25.4

Longitudinal Tests

Four types of footwear were compared to determine if the footwear influenced longitudinal test results. Only tests which had leg flail were included in the analysis (*Table 7*), which included the tests with sneakers with the modified leg position. To quantify testing variability, the mil spec tests were compared against each other. To evaluate the effect of the alternate footwear types, these results were then compared with the mil spec tests. Head path was used for comparison since it provides the data for the most critical aspect of occupant kinematics. Floor load was also used in comparison as it is the most direct measurement of the footwear and floor interaction.

Table 7: Tests Discussed in the Effect of Footwear.

Test	Clothing	Footwear
A22003	100% Cotton	Mil Spec
A22009	100% Cotton	Mil Spec
A21011	100% Cotton	Boots
A21012	100% Cotton	Boots
A22002	100% Cotton	Boots
A21008	100% Cotton	Bowling
A21009	100% Cotton	Bowling
A22001	100% Cotton	Bowling
A22004	100% Cotton	Bowling
A22005	100% Cotton	Sneakers
A22011	60%/40% Poly	Sneakers
A22012	60%/40% Poly	Sneakers

Mil Spec Comparison Tests (Mil Spec vs. Mil Spec)

Three 100% cotton clothing with mil spec footwear (the “baseline” apparel combination) tests were run: A22003, A22006, and A22009. Test A22006 had limited leg flail and therefore was excluded.

Head Path

The head CG initial position, maximum X-position, and minimum Z-position values are presented in *Table 8 for the two tests with the mil spec that had full leg flail*. There was only a change of 0.1 in. in head excursion (maximum X-position), achieved within 1 ms between tests. There was a 1.5 in. difference in the minimum Z-position, occurring within 4 ms between tests.

Table 8: Head Path Values (Baseline).

Test	Clothing	Footwear	X-Position at t=0 (in.)	Z-Position at t=0 (in.)	Max X-Position (in.)	Time (ms)	Min Z-Position (in.)	Time (ms)
A22003	100% Cotton	Mil Spec	5.8	45.2	44.5	175	6	222
A22009	100% Cotton	Mil Spec	6.1	45.8	44.6	174	7.5	218

The head path plots for X-position versus Z-position for tests A22003 and A22009 are shown in *Figure 15*. Both curves follow the same path until the head reaches the maximum X-position, where the curves start to deviate and end up at the 1.5 in. difference in the minimum Z-position. The head path data is plotted for both X-position versus time and Z-position versus time (*Figure 16*). To evaluate the difference in the shape of the two curves, the Sprague and Geer's (S&G) method was applied to calculate the shape error between data curves. This method is identified in SAE International ARP5765B where it is used to compare physical test results with computer modeling results (SAE International, 2021). The results of the shape error analysis are categorized as follows: an error percentage ranging from 0% to 4% is deemed excellent; 4% to 10% is considered good; 10% to 20% is classified as fair; 20% to 40% is categorized as poor; and any error exceeding 40% is considered very poor (Moorcroft, 2007). Test A22003 was chosen as the baseline test for purposes of this calculation. The total comprehensive error (shape error) was calculated between the two curves for both X-position versus time and Z-position versus time, resulting in 1.3% and 3.4% difference, respectively.

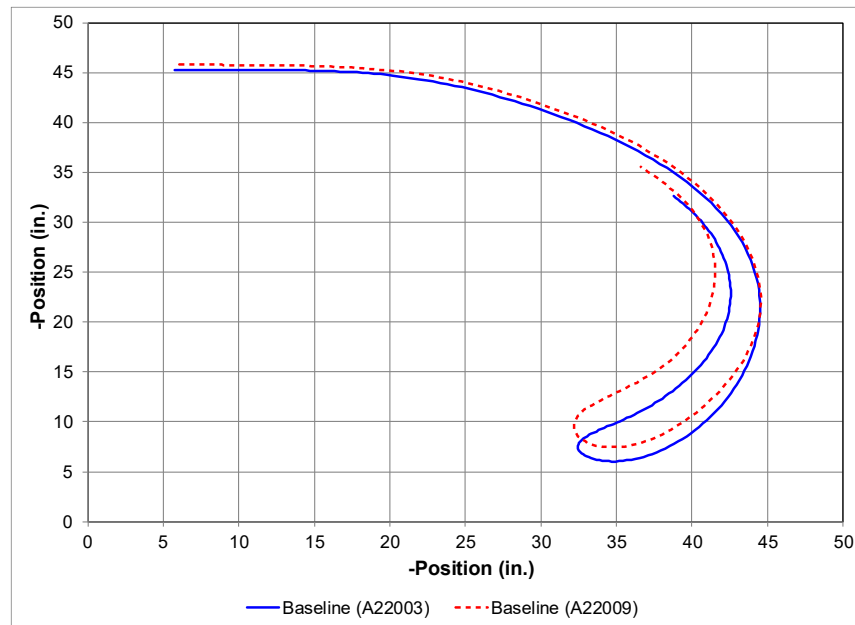


Figure 15: Head Path for Baseline: X-position vs Z-Position.

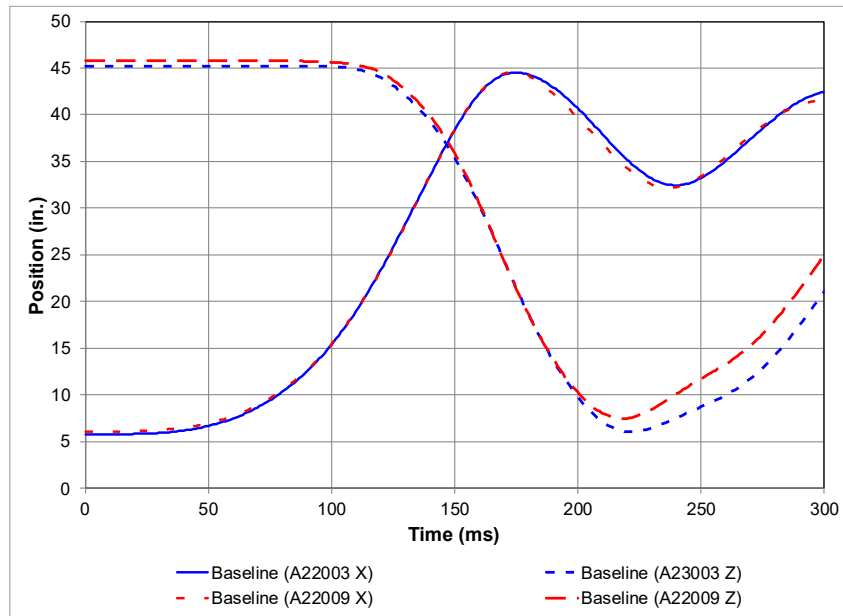


Figure 16: Head Path for Baseline: X and Z-Position vs. Time.

Floor Load

Figure 17 is a plot of floor loads in the X-direction versus time for tests A22003 and A22009. The two plots have a similar shape, which could be considered a double peak or a flat top. While the initial onset is the same for both tests, test A22003 peaks earlier and at a lower magnitude than test A22009. The curves diverge more noticeably when reaching their second peaks due to the left heel maintaining contact for the additional time in test A22009 and achieving the highest peak load at 266 lb. The shape error for the floor loads were calculated for the first 300 ms resulting in a difference of 31.7%.

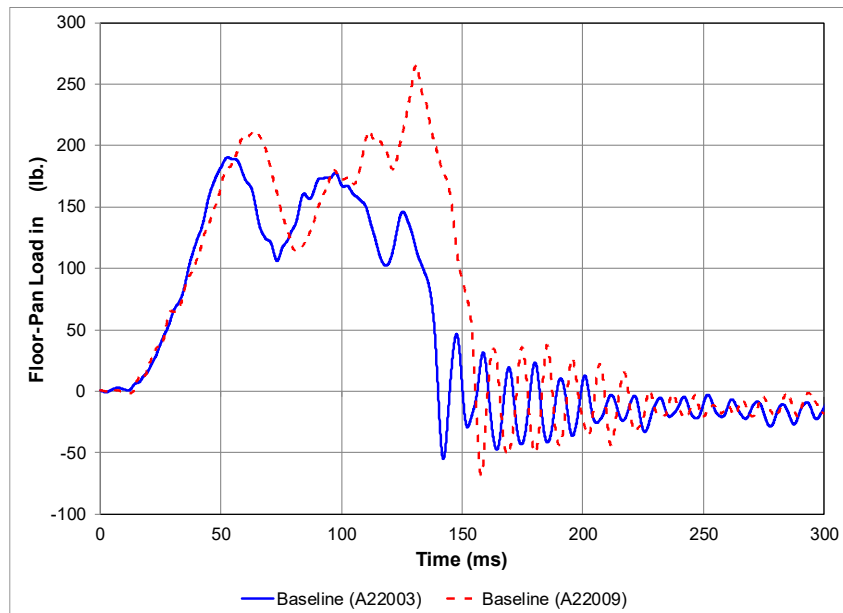


Figure 17: Floor Load in X-Direction for Baseline.

Boots vs Mil Spec

Three tests with the boots and two mil spec tests were used for this comparison. Only tests which had full leg flail were included in the analysis.

Head Path

The ATD's head center of gravity's initial position, maximum head excursion in X, and minimum position in Z are presented in Table 9. The range of values for head excursion in X for the boots was 44.7 in. to 45.6 in. and the range for the mil spec was 44.5 in. to 44.6 in. The head excursion for all the boots tests exceeds the mil spec values in the X-position. The minimum Z-position achieved with boots ranged from 5.9 to 7.2 in. while the mil spec ranged from 6.0 to 7.5 in. The head paths for the boots and the mil spec are plotted in [Figure 18](#) (Z-position vs. X-position), [Figure 19](#) (X-position vs. time), and [Figure 20](#) (Z-position vs. time). The shape error was calculated for the X-position vs time for tests A22003 and A21011, resulting in a 2.0% difference. The shape error was also calculated for the same tests for Z-position vs. time, resulting in a difference of 4.1%.

Test A22003 was selected as the baseline for the shape error calculation since it had the lowest head path values of the two baseline tests, and it was retained as reference for all other comparisons (i.e., floor loads, seat-pan loads, etc.) to maintain consistency. Test A21011 was chosen because it showed the greatest variation from A22003, as determined by a visual check. This methodology of selecting the curve that deviated most from A22003 based on visual inspection was consistently applied throughout the report to choose curves for the S&G calculations. Since either baseline test (A22003 or A22009) could have been used, additional shape error calculations were performed to evaluate the impact of this choice: A21011 compared to A22003 resulted in a 1.99% error, A22003 to A21011 2.00%, A22009 to A21011 4.96%, and A21011 to A22009 4.91%. While calculating all four possible pairwise combinations would provide more completeness, it would also significantly increase the data volume with minimal effect on the results.

Table 9: Head Path Values (Boots and Mil Spec).

Test	Clothing	Footwear	X- Position at t=0 (in.)	Z- Position at t=0 (in.)	Max X- Position (in.)	Time (ms)	Min Z- Position (in.)	Time (ms)
A22003	100% Cotton	Mil Spec	5.8	45.2	44.5	175	6.0	222
A22009	100% Cotton	Mil Spec	6.1	45.8	44.6	174	7.5	218
A21011	100% Cotton	Boots	5.8	45.5	45.0	173	7.2	212
A21012	100% Cotton	Boots	4.9	45.0	45.6	174	5.9	212
A22002	100% Cotton	Boots	5.0	44.7	44.7	174	6.6	215

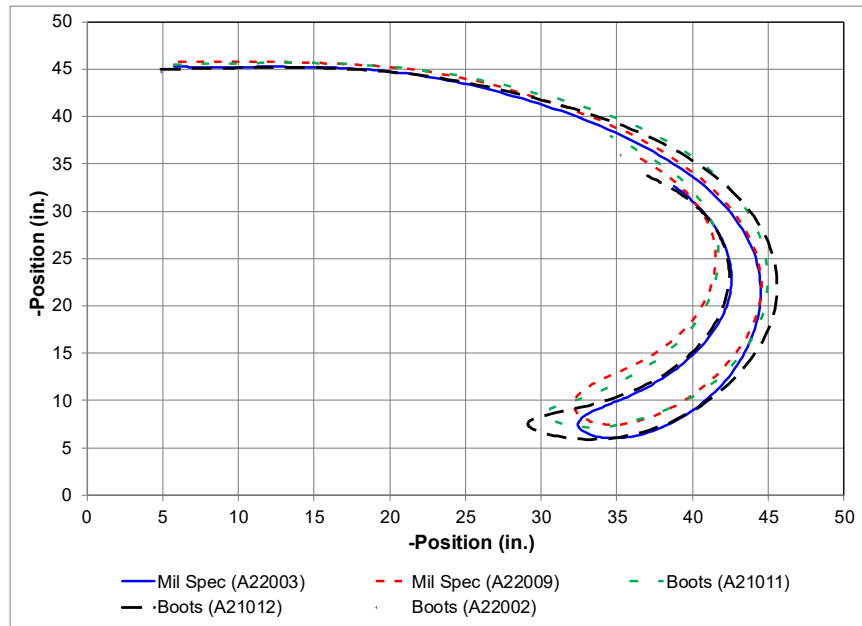


Figure 18: Head Path for Boots and Mil Spec: X-position vs Z-Position.

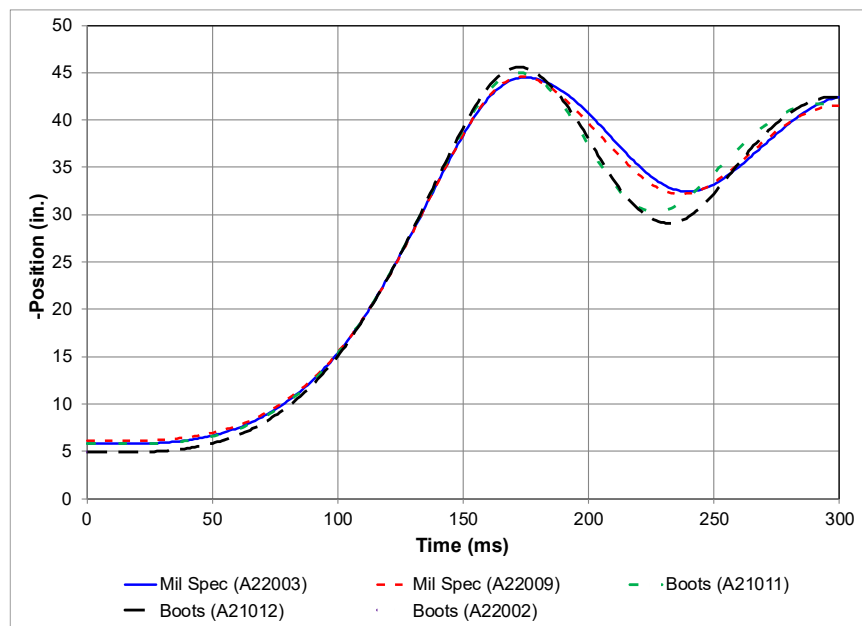


Figure 19: Head Path for Boots and Mil Spec: X-Position vs Time.

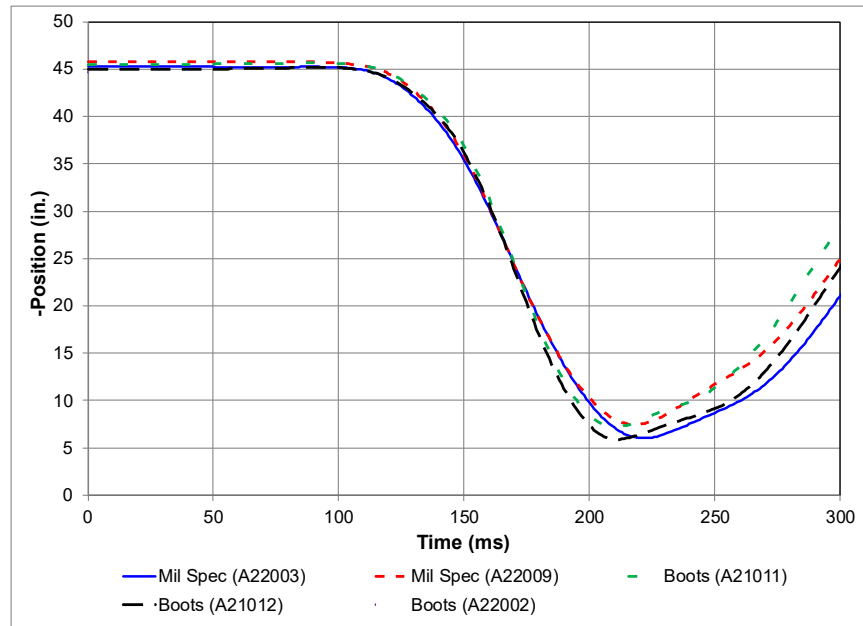


Figure 20: Head Path for Boots and Mil Spec: Z-Position vs Time.

Floor load

The tests with the boots achieved similar initial floor load peaks, with values ranging from 125 to 129 lb. ([Figure 21](#)). The difference in the initial peak between tests A21011 (boots) and A22009 (mil spec) was 80 lb. Test A22002 was the only boots test to achieve a second peak. The video from test A22002 showed the left foot clearing the floor pan, then the right foot loading the floor pan (achieving the second peak), and then the right foot ending contact with the floor pan (right picture in [Figure 23](#)). The boots clear the floor-pan at the following times: 119 ms (A21011), 121 ms (A21012), and 130 ms (A22002), whereas the mil spec cleared the floor at 148 ms (A22003) and 154 (A22009). Even with the second loading of the foot in test A22002, all the tests with the boots cleared the floor quicker than mil spec tests. The ATD position at maximum floor load and the last frame with the foot in contact with the floor pan are shown in [Figure 22](#) (A21011), [Figure 23](#) (A22002), and [Figure 24](#) (A22009). The comparison of these five tests revealed that the mil spec footwear achieved higher floor-pan loads with longer durations than the boots. The shape error was calculated between A22003 and A21011, which resulted in a 53.6% difference.

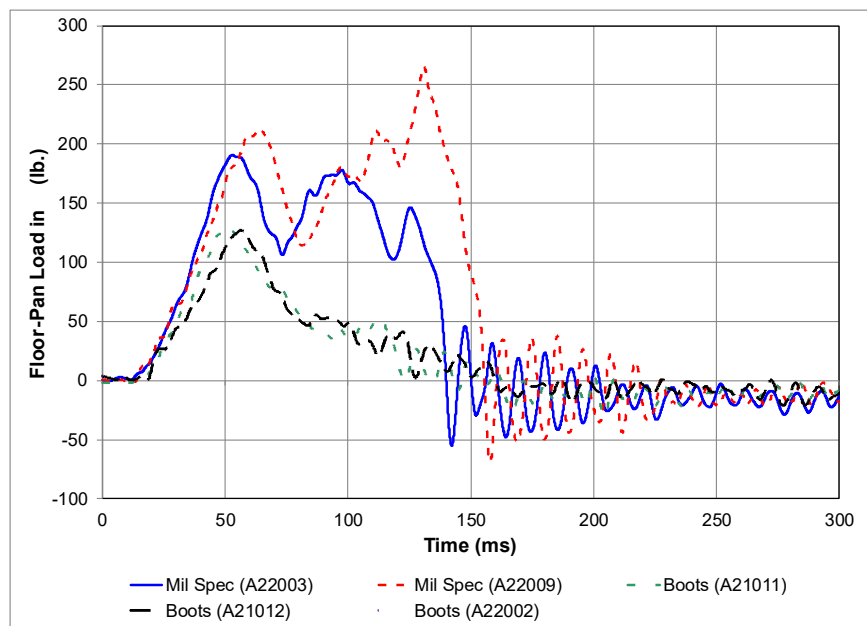


Figure 21: Floor-Pan Loads in X-Direction (Boots vs Mil Spec).

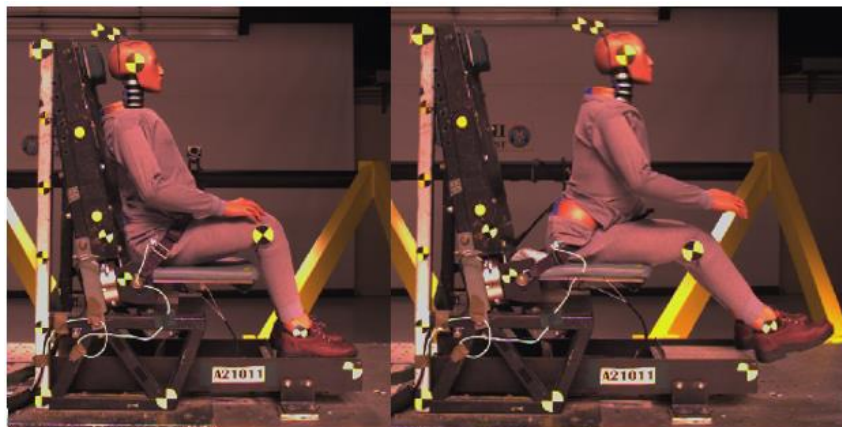


Figure 22: A21011 (Boots) Peak Load Floor-Pan Load at 52 ms (Left) and Last Frame at 119 ms (Right).



Figure 23: A22002 (Boots) Peak Load Floor-Pan Load at 62 ms (Left) and Last Frame at 130 ms (Right).

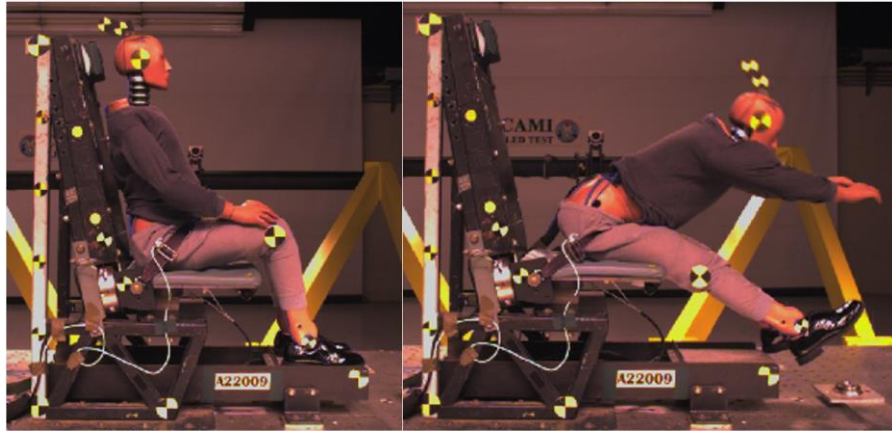


Figure 24: A22009 (Mil Spec) Peak Load Floor-Pan Load at 64 ms (Left) and Last Frame at 154 ms (Right).

Bowling Shoe vs Mil Spec

The four bowling shoe tests with the 100% cotton clothing were compared with two mil spec tests. Only tests which had full leg flail were included in the analysis.

Head Path

Head-path data for the initial position, maximum head excursion in X, and minimum position in Z, including corresponding times, are presented in [Table 10](#). The range of values for head excursion in X for the bowling shoe was 44.2 in. to 45.2 in. and the range for the mil spec was 44.5 in. to 44.6 in. The range of minimum values of head position in Z were 5.4 in. to 6.3 in. for the bowling shoe and 6.0 in. to 7.5 in. for the mil spec.

Table 10: Head Path Values (Bowling and Mil Spec).

Test	Clothing	Footwear	X-Position at t=0 (in.)	Z-Position at t=0 (in.)	Max X-Position (in.)	Time (ms)	Min Z-Position (in.)	Time (ms)
A22003	100% Cotton	Mil Spec	5.8	45.2	44.5	175	6.0	222
A22009	100% Cotton	Mil Spec	6.1	45.8	44.6	174	7.5	218
A21008	100% Cotton	Bowling	5.7	45.4	44.8	173	7.2	213
A21009	100% Cotton	Bowling	5.4	45.3	45.1	173	5.4	211
A22001	100% Cotton	Bowling	5.2	44.9	44.2	174	6.3	219
A22004	100% Cotton	Bowling	5.2	45.2	45.2	175	5.6	220

The head paths for four bowling shoe and two mil spec tests are plotted in [Figure 25](#) (Z-position vs X-position), [Figure 26](#) (X-position vs time), and [Figure 27](#) (Z-position vs time). Tests A22003 and A22001 were selected to calculate the shape error for both X-position versus time (1.93% difference) and Z-position versus time (2.11% difference).

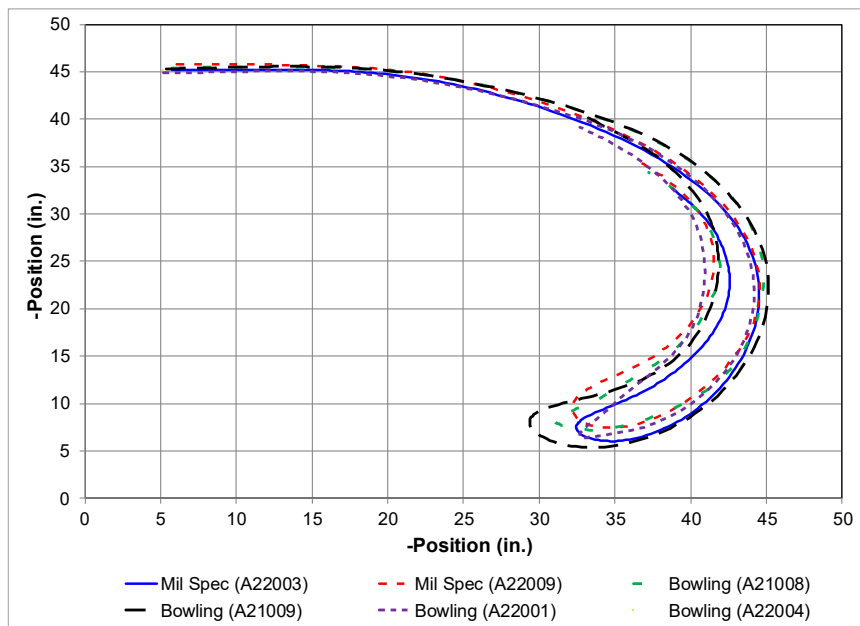


Figure 25: Head Path for Bowling Shoe and Mil Spec: X-Position vs. Z-Position.

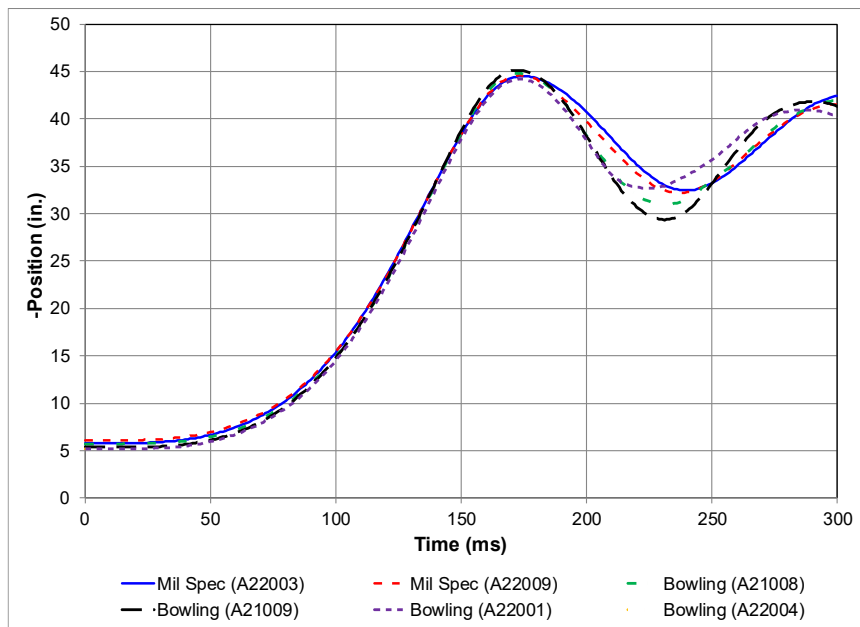


Figure 26: Head Path for Bowling Shoe and Mil Spec: X-Position vs. Time.

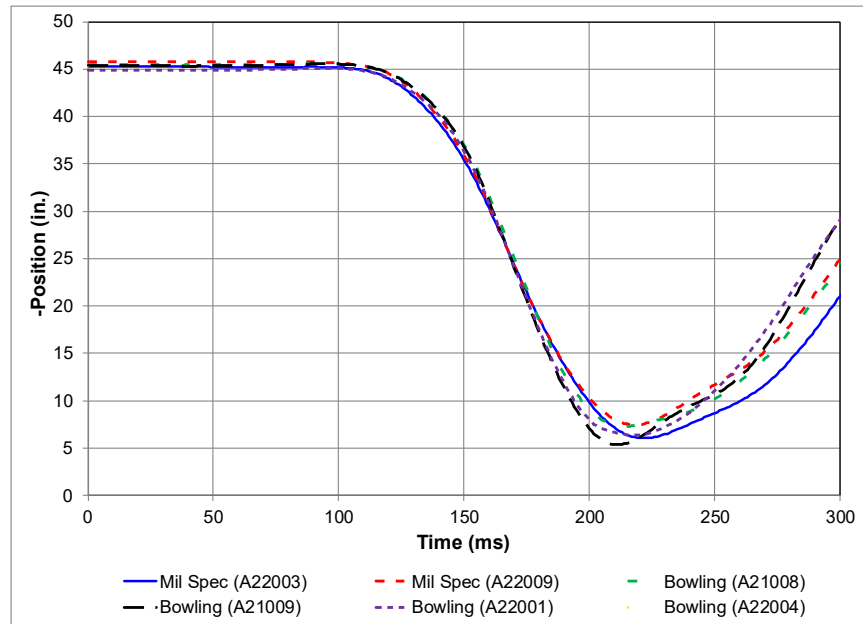


Figure 27: Head Path for Bowling Shoe and Mil Spec: Z-Position vs. Time.

Floor load

Figure 28 has the plots of the X-direction floor load for the six tests. All the bowling shoe loads follow the same curve. The bowling shoe peaks are approximately one-third of the mil spec initial peaks. The highest peak load achieved with the bowling shoe was 76 lb. in test A21008. The mil spec achieved an initial peak load of 191 lb. in test A22003. Figure 29 shows two still images from test A22001: ATD's position at peak floor load and the last frame of the shoe in contact with the floor pan. The four bowling shoe tests clear the floor-pan at between 114 and 115 ms, whereas the mil spec cleared the floor at 148 ms (A22003) and 154 (A22009). Shape error was calculated between the load curves of tests A22003 and A22001 with a resulting error of 71.3%.

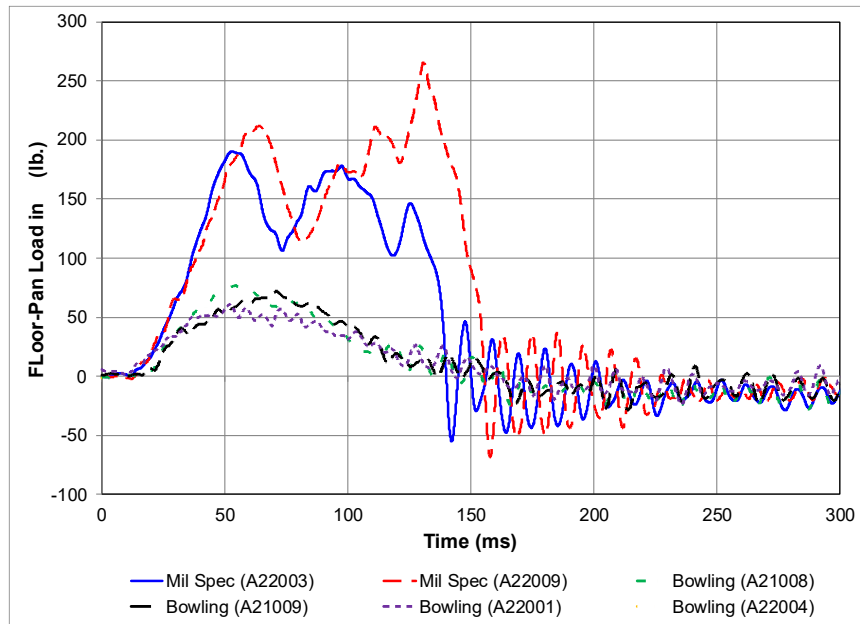


Figure 28: Floor Load in X-Direction (Bowling Shoe and Mil Spec).



Figure 29: A22001 Peak Load Floor Load at 51 ms (Left) and Last Frame at 115 ms (Right).

Sneakers vs Mil Spec

Three tests with sneakers (A22005, A22011, and A22012) and two mil spec tests (A22003 and A22009) were used for this comparison. Only tests which had leg flail were included in the analysis. Test A22005 had 100% cotton clothing, which matched the tests with the mil spec shoes, while tests A22011 and A22012 used 60/40 clothing to enable multiple sneaker comparisons.

Head Path

Table 11 has the initial position, maximum head excursion in X, and minimum position in Z, with their respective times. The range of values for head excursion in X for the sneakers was 44.1 in. to 45.1 in. and the range for the mil spec was 44.5 in. to 44.6 in. The range of values for minimum head position in Z for the sneakers was 6.6 in. to 7.0 in. and the mil spec was 6.0 in. to 7.5 in.

Table 11: Head Path Values (Sneakers and Mil Spec).

Test	Clothing	Footwear	X-Position at t=0 (in.)	Z-Position at t=0 (in.)	Max X-Position (in.)	Time (ms)	Min Z-Position (in.)	Time (ms)
A22003	100% Cotton	Mil Spec	5.8	45.2	44.5	175	6.0	222
A22009	100% Cotton	Mil Spec	6.1	45.8	44.6	174	7.5	218
A22005	100% Cotton	Sneakers	5.6	45.2	45.1	175	6.6	221
A22011	60%/40% Poly	Sneakers	5.6	45.4	44.9	175	6.9	220
A22012	60%/40% Poly	Sneakers	5.8	45.4	44.1	174	7.0	219

The head paths for the sneakers and mil spec tests are plotted in Figure 30 (X-position vs. Z-position), Figure 31 (X-position vs. time), and Figure 32 (Z-position vs. time). In both Figure 30 and Figure 31 the curves for the sneakers fall between the two mil spec curves. Tests A22003 and A22005 were selected to calculate the shape error for both X-position versus time and Z-position versus time, resulting in a difference of 0.5% and 0.8%, respectively.

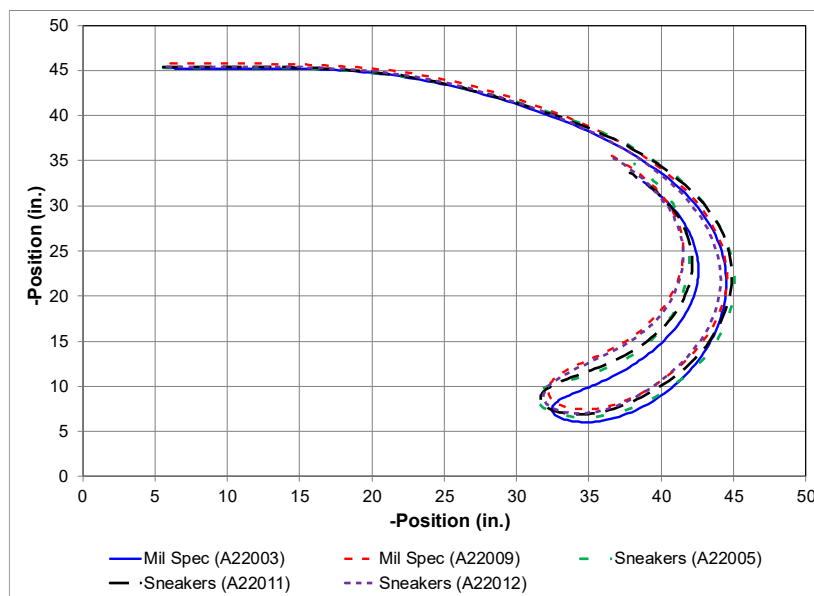


Figure 30: Head Path for Sneakers and Mil Spec: X-Position vs Z-Position.

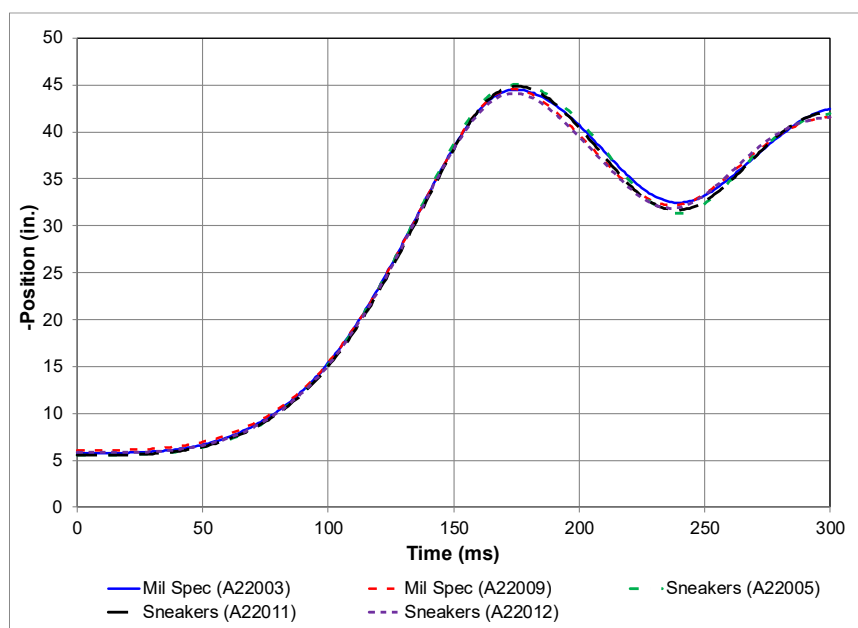


Figure 31: Head Path for Sneakers and Mil Spec: X-Position vs. Time.

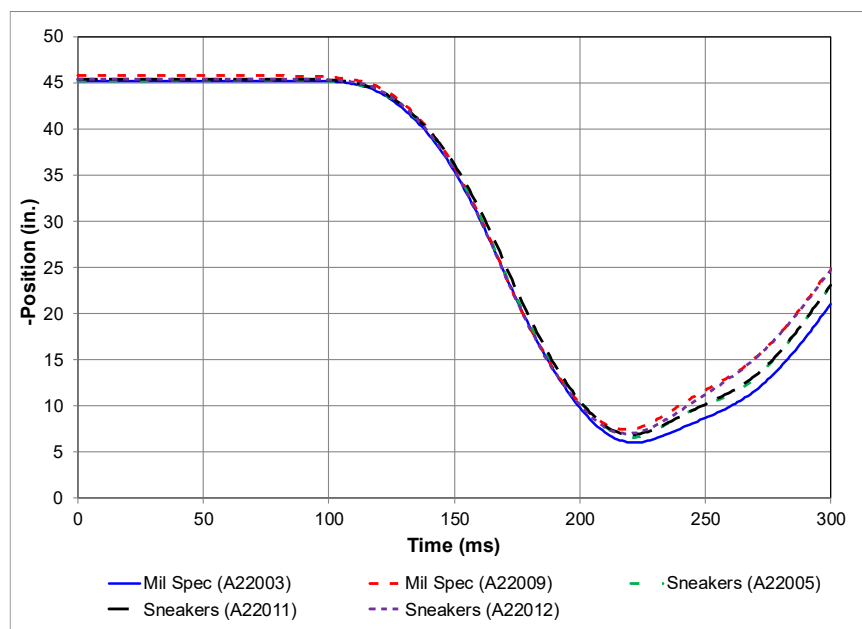


Figure 32: Head Path for Sneakers and Mil Spec: Z-Position vs. Time.

Floor load

Figure 33 has the plots of the five floor loads, in the X-direction. The peak load achieved with the sneakers was 241 lb. in test A22011. The peak load for the sneakers was 50 lb. more than the peak load of the mil spec (191 lb.) achieved in test A22003. The feet were moved forward two inches of the heel stop in the three tests with the sneakers, and results show that the initial peak

loads were higher and a longer duration, than the mil spec footwear. Figure 34 has images from test A22011 showing the ATD's position at peak seat-pan load (75 ms) and the last frame with the shoe in contact with the floor pan (141 ms). The sneakers clear the floor-pan in the other two tests at the following times: 132 ms (A22005) and 146 ms (A22012), whereas the mil spec cleared the floor at 148 ms (A22003) and 154 (A22009). The shape error was calculated between A22003 and A22005, resulting in a difference of 21.8%.

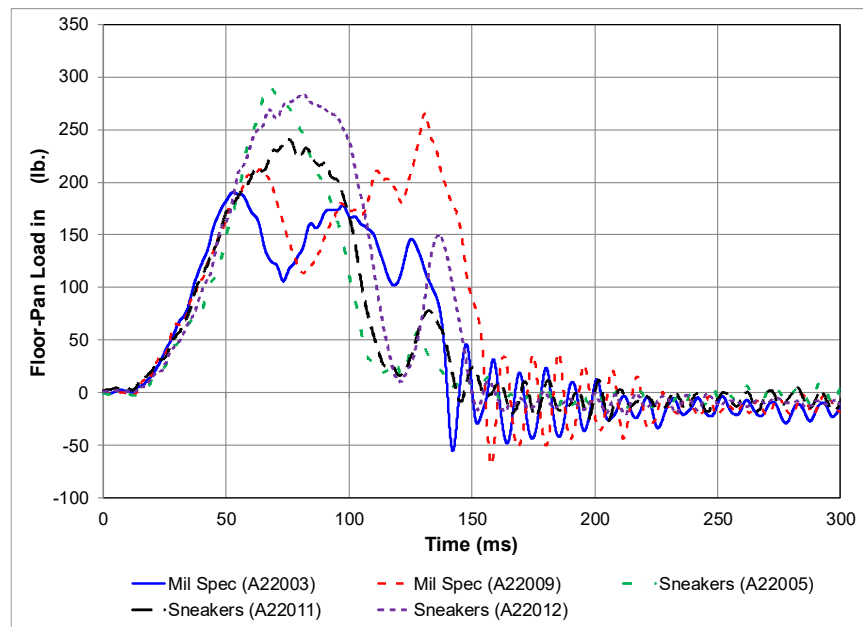


Figure 33: Floor-Pan Loads in the X-Direction (Sneakers and Mil Spec).

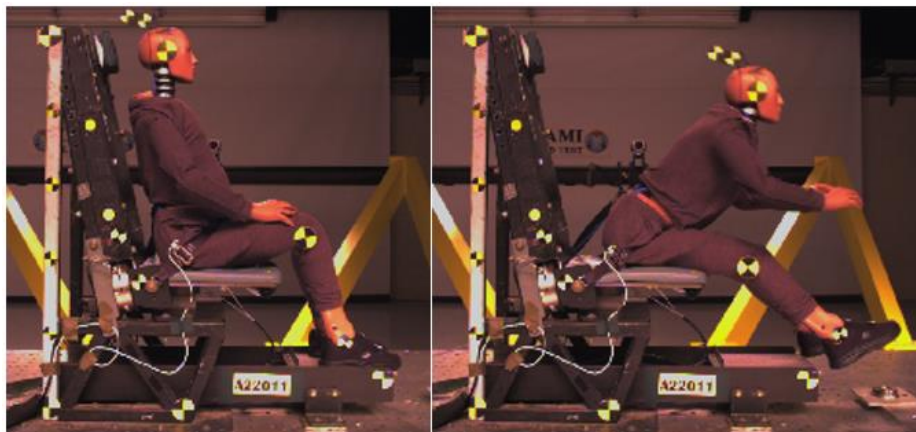


Figure 34: Photo of Peak Load in A22011 (Sneakers) at 75 ms (Left) and Last Photo with Feet on Floor at 141 ms (Right).

Vertical Tests

Vertical tests were run to determine whether the footwear influences the ATD's interaction with the seat and floor in this test configuration. Three tests (A22015, A22016 and A22017) were run with the boots, which had the hardest sole material and the highest heel (1.85 in. on average). Three tests (A22018, A22019, and A22020) were run with the sneakers, which had the softest sole and the second shortest heel (1.28 in. on average). All vertical tests were run with 100% cotton clothing. The mil-spec and bowling shoes were not included in this test series because their sole stiffness fell between that of the softest and hardest shoes evaluated. The intention was to focus on the performance extremes of sole stiffness to facilitate comparisons.

ATD pretest positions were collected with the CMM to capture the leg angle. The leg angle is the angle the leg makes with respect to a vertical line, perpendicular to the floor pan (*Figure 35*). The figure also shows the X-Z coordinate system. The leg angles for the tests with sneakers ranged from 17.3° to 19.6°. The leg angle for the boots was 16.3° to 18.6°. The change in leg angle between the footwear was the result of the thick aft edge of the sole on the sneakers which pushed the ankle further forward.

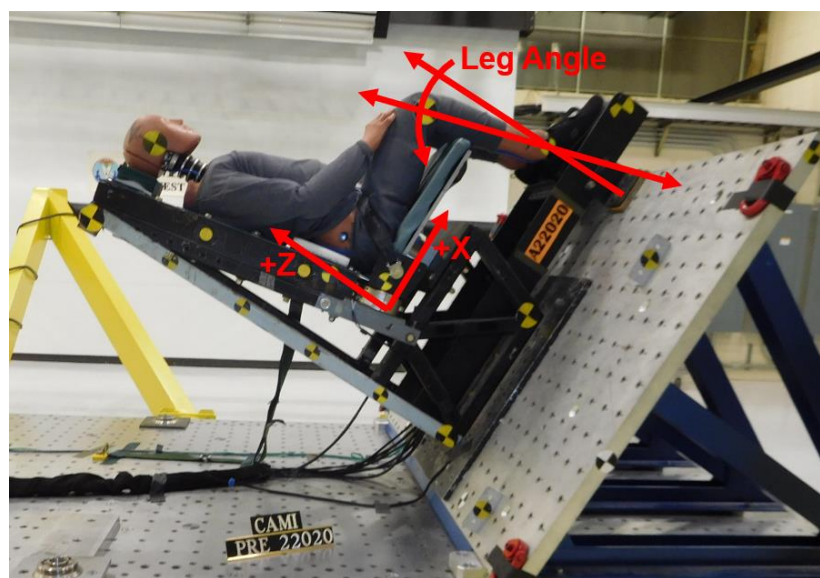


Figure 35: Leg Angle Dimension for the Vertical Tests and CMM Coordinate System.

The peak loads for the lumbar spine, seat pan, and floor pan are presented in *Table 12*. The average normalized peak lumbar load for the sneakers was -1240 lb., while the average for the boots was -1222 lb. This falls within the range seen in previous research which quantified lumbar load variability of ~160 lb. for 2 in. cushions and as much as 340 lb. for thicker cushions. The highest variability in the peak loads was in the seat-pan loads (283 lb.). The range in the peak floor loads was 33 lb. across all six tests. The normalized lumbar load is calculated by dividing the desired peak acceleration by the actual peak acceleration and multiplying it by the measured lumbar load. This adjustment is done to compensate for small differences in test severity when comparing results (DeWeese et al., 2021).

Table 12: Peak Load Cell Value for Lumbar, Seat-Pan and Floor Load.

Test	Footwear	Normalized Peak Lumbar Load (lb.)	Peak Seat-Pan Load (lb.)	Peak Floor Load (lb.)
A22015	Sneakers	-1188	2228	1043
A22016	Sneakers	-1223	2454	1063
A22017	Sneakers	-1309	2512	1054
A22018	Boots	-1225	2409	1031
A22019	Boots	-1212	2328	1064
A22020	Boots	-1230	2384	1052

Figure 36, *Figure 37*, and *Figure 38* show the load in the Z-direction for the lumbar, seat-pan, and floor loads, respectively. The lumbar load and seat-pan load curves have the same shape, with only minor differences in the peak. The floor load curves overlay except for local peaks between 45-75 ms in two of the tests with the sneakers (A22018 and A22019). These local peaks had a minimal effect on the magnitude and timing of the peaks.

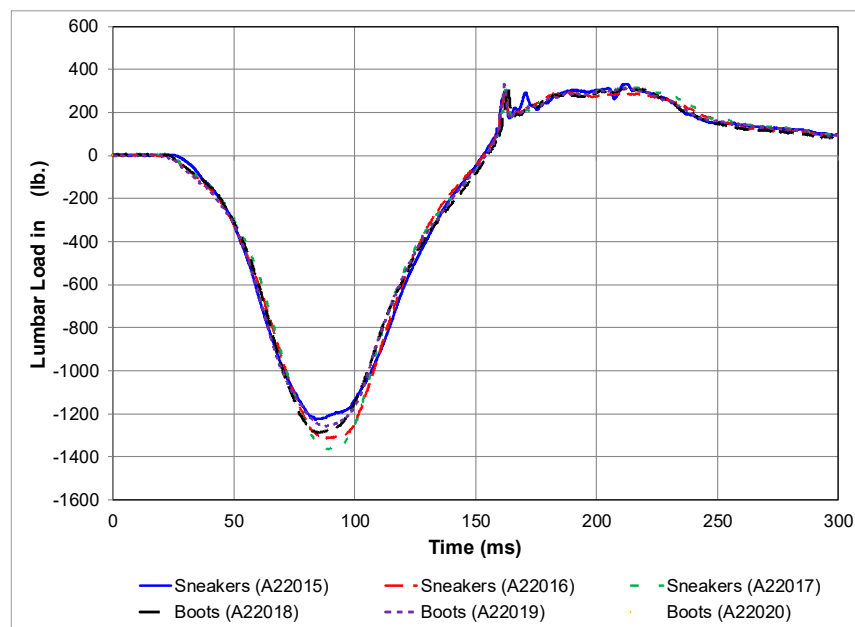


Figure 36: Lumbar Loads in Z-Direction for Vertical Tests.

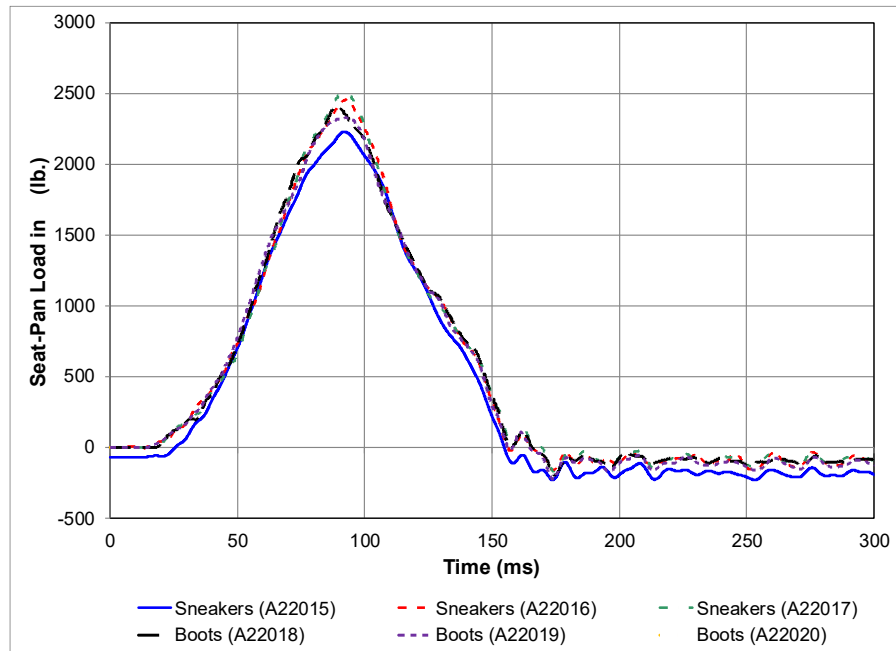


Figure 37: Seat-Pan Load in Z-Direction for Vertical Tests.

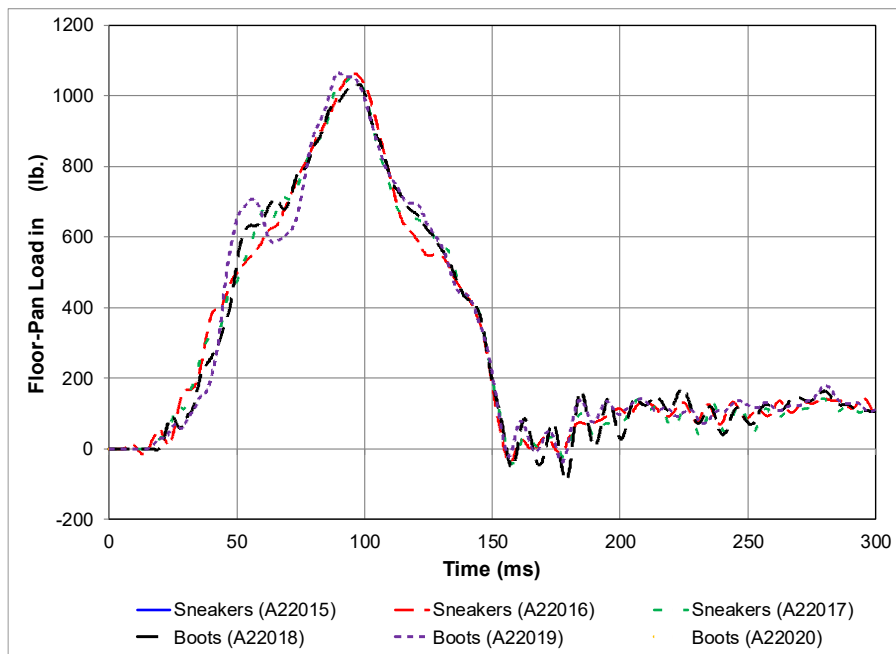


Figure 38: Floor-Pan Load in Z-Direction for Vertical Tests.

Summary - Effect of Footwear

In tests with the mil spec, the variance in maximum head X-position was 0.1 in. while the maximum X-position in the other three footwear types had a variance between 0.9 in. and 1.1 in. Based on the similarities of the other data in this report it is assumed that the scatter of the mil spec would

be about 1 in. if additional data were collected. *Figure 39* is a bar chart of the average maximum head excursion for each shoe combination along with error bars based on the observed range. For the mil spec, the assumed error of ± 0.5 in. is shown with the red horizontal lines for the maximum and minimum. The assumed mil spec range incorporates almost all the of the sneaker and bowling shoe and overlays ~50% of the bowling shoe range. Based on this data, we conclude that with full leg flail, the footwear type has at most a minor impact on the occupant response in a Part 25 longitudinal test. The use of alternate footwear had minimal effect on the head path. For vertical testing, lumbar loads showed no difference between the hardest and softest soles.

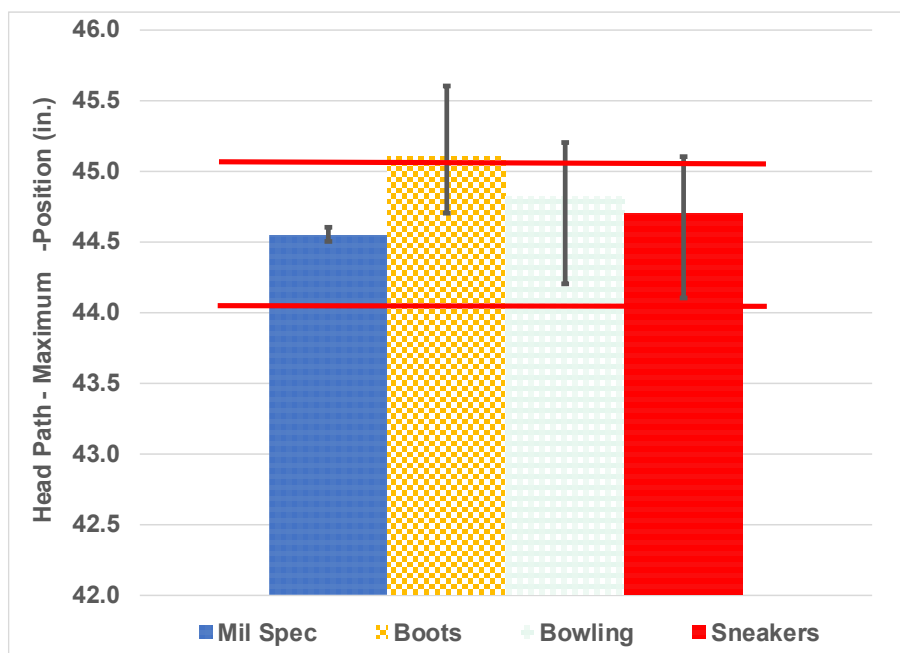


Figure 39: Footwear Head Excursion Average and Range Bar Chart.

Effect of Clothing in Longitudinal Tests

Three types of clothing were run in the longitudinal test series: 100% cotton, 60% cotton & 40% polyester (abbreviated 60%/40% poly or 60/40), and 92% polyester & 8% spandex (abbreviated 92%/8% poly or 92/8) (*Table 13*). The variability in testing was determined by comparing the 100% cotton tests against each other. Results from the two alternative clothing types were then compared to the 100% cotton tests. Head path was evaluated since it is the most critical aspect of occupant kinematics for a longitudinal test and should capture the global influence of friction. The seat-pan load was used as an indicator of the local effect of friction between the clothing and seat bottom cushion due to the forward movement of the ATD. Seat pan loads were analyzed over a period from 0 to 300 milliseconds; however, the most informative time frame for assessing the clothing is from 0 to approximately 110 milliseconds during the ATD's initial forward movement. Additionally, while the peaks observed later in the tests were compared, they may be more closely related to the overall ATD motion rather than directly correlated with the clothing. The pelvis angle and the seat belt restraint loads were used to determine the effect of friction between the clothing material and the belt.

Table 13: Tests Discussed in the Effect of Clothing.

Test	Clothing	Footwear
A22003	100% Cotton	Mil Spec
A22009	100% Cotton	Mil Spec
A22011	60%/40% Poly	Sneakers
A22012	60%/40% Poly	Sneakers
A21013	92%/8% Poly	Bowling
A21014	92%/8% Poly	Bowling
A22014	92%/8% Poly	Bowling

100% Cotton Comparison Tests (100% Cotton vs. 100% Cotton)

Tests A22003 and A22009 represent the clothing and footwear outlined in AS8049D; 100% cotton clothing with the mil spec. These tests represent the “baseline” combination that will be used to compare the result of the other two clothing types. As discussed in detail in section “Effect of Leg Flail in Longitudinal Tests” any test with limited ATD flail was not used in these data comparisons.

Head Path

The head path for this combination of clothes and footwear are the same tests (A22003 and A22009) covered in footwear section “Head Path”.

Seat-Pan Loads

Figure 10 shows the ATD position during the three primary seat-pan load peaks for test A22003. The seat-pan loads in the X-direction for tests A22003 and A22009 are plotted in Figure 40. Both curves achieve their maximum value in the positive direction at ~110 ms, while the ATD is sliding forward. The load in the positive X-direction is the effect of the friction between the occupant and the seat. The first negative peak for both curves occurs at ~160 ms. The corresponding photo at 160 ms shows that the pan is bending down and the ATD’s thighs are angled downward, pushing the seat pan rearward. A similar thigh position is seen at ~220 ms, and higher loads were achieved, due to the chest impacting the thigh further pushing the seat pan rearward. The shape error was calculated up to 300 ms and the result was 13.9%.



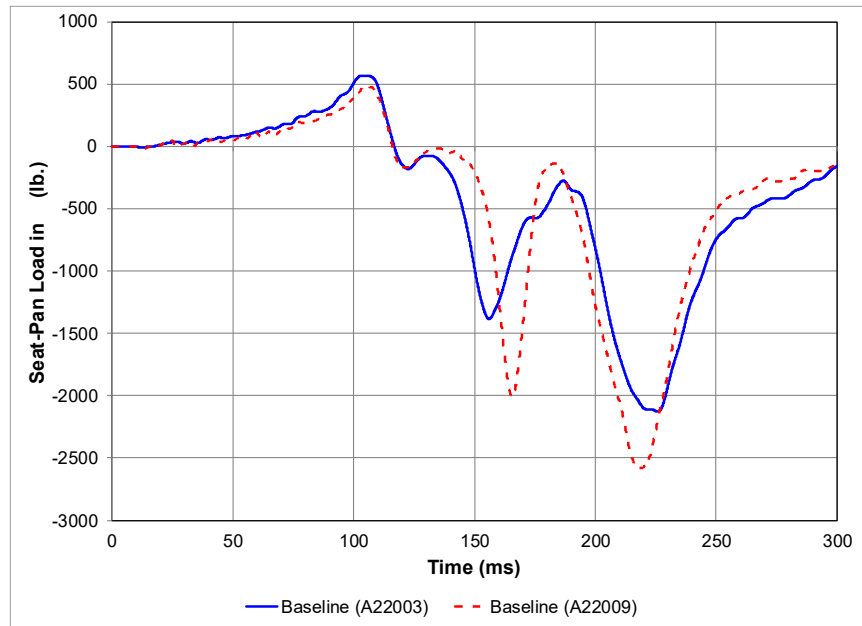


Figure 40: Seat-Pan Force in the X-Direction (Baseline).

Seat Belt Restraint Loads

The seat belt-transducer loads for the 100% cotton tests are plotted in [Figure 41](#). The belt load curves show that two peaks were achieved. The first peak occurs at approximately 110 ms and the second peak occurs at 160 ms. Both curves reach their maximum value during the second peak. The shape error calculated between the two curves was 22.3%.

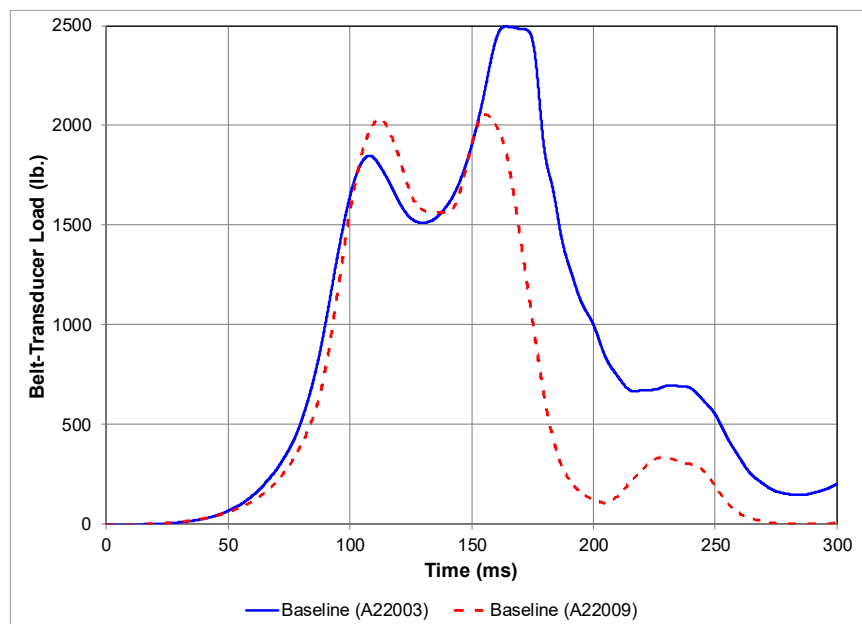


Figure 41: Belt-Transducer Loads for Baseline.

Pelvis Angle

The pelvis angle about the Y-axis for the baseline tests are plotted in [Figure 42](#). The pelvis angle was calculated using the angular velocity data from the pelvis angular rate sensor integrated over time. The position of the upper vertical H-point target was not collected prior to every test; thus, the angle data indicates relative change in angle, not the absolute angle. The peak rotation achieved in test A22003 was -85.0 degrees and test A22009 was -74.0 degrees. The shape error calculated between the two curves for 0 to 300 ms was 16.8%.

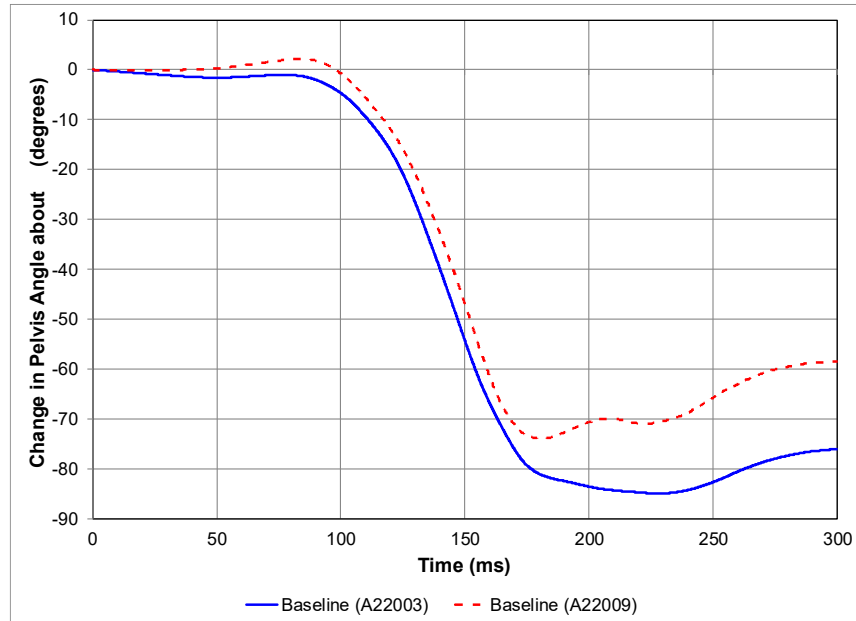


Figure 42: Change in Pelvis Angle about Y-Axis for Baseline.

60% Cotton/40% Polyester vs. 100% Cotton Clothing

Three total tests were run with the 60% cotton/40% polyester (60/40) clothing with sneakers. Two of the three tests, A22011 and A22012, achieved full leg flail. These two 60/40 tests were compared with the 100% cotton tests, A22003 and A22009.

Head Path

Head-path data for the four tests is provided in [Table 14](#). The maximum X values for the 60/40 clothing range from 44.1 to 44.9 in., placing the baseline cotton clothing values of 44.5 to 44.6 in. nearly in the middle. The minimum Z-values for the 60/40 tests fall between the values for the baseline combination.

Table 14: Head Path Values (60/40 and Cotton).

Test	Clothing	Footwear	X-Position at t=0 (in.)	Z-Position at t=0 (in.)	Max X-Position (in.)	Time (ms)	Min Z-Position (in.)	Time (ms)
A22003	100% Cotton	Mil Spec	5.8	45.2	44.5	175	6.0	222
A22009	100% Cotton	Mil Spec	6.1	45.8	44.6	174	7.5	218
A22011	60%/40% Poly	Sneakers	5.6	45.4	44.9	175	6.9	220
A22012	60%/40% Poly	Sneakers	5.8	45.4	44.1	174	7.0	219

The head path X-position versus the Z-position for the four tests is plotted in [Figure 43](#). The head path X-position versus time and the Z-position versus time are both plotted [Figure 44](#) and [Figure 45](#), respectively. These plots show good agreement until around 225 ms, after which divergence begins, most notably in the Z-direction. The shape error was calculated between A22003 and A22012 was 1.1% for the X-position versus time and 1.6% for the Z-position versus time.

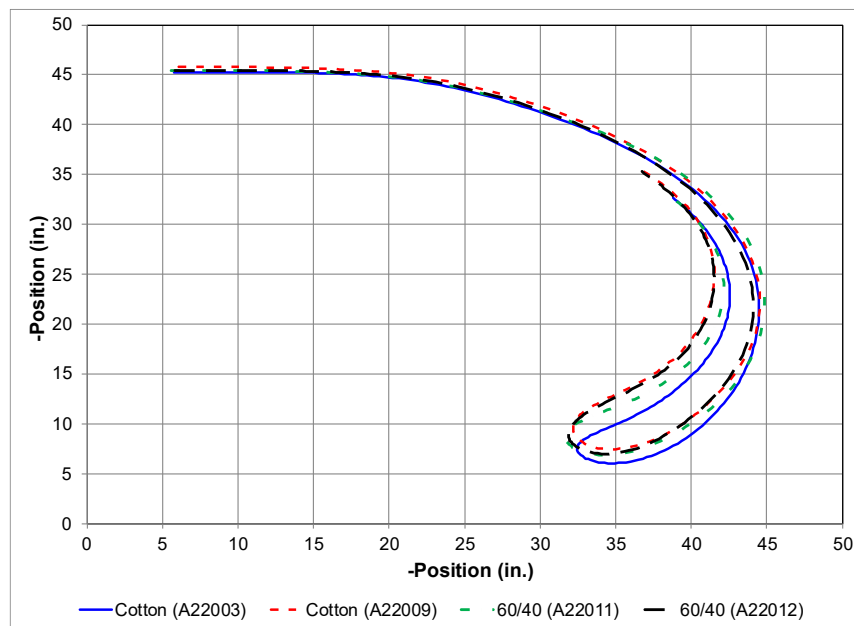


Figure 43: Head Path for 60/40 and Cotton: X-Position vs. Z-Position.

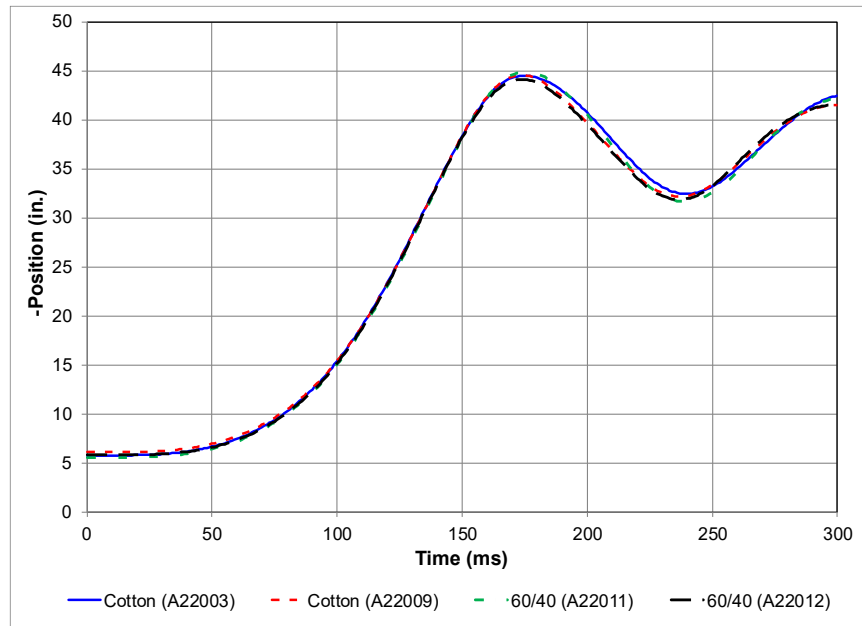


Figure 44: Head Path for 60/40 and Cotton: X-Position vs. Time.

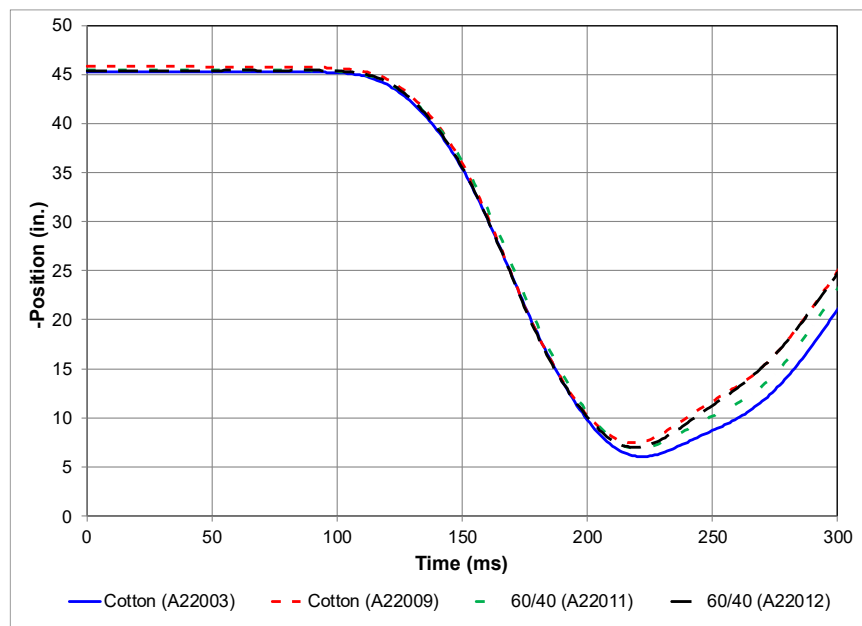


Figure 45: Head Path for 60/40 and Baseline: Z-Position vs. Time.

Seat-Pan Loads

The four seat-pan load curves follow similar paths for the duration of the test ([Figure 46](#)). The variance between the curves occurs at the three peaks. The maximum positive peak occurred when the ATD is sliding forward across the seat pan. The two peaks, in the negative direction occurred when the ATD's thighs are angled downward, thus pushing the seat pan rearward. The

peak loads and their respective times are provided in [Table 15](#). The shape error was calculated between tests A22003 and A22012, from 0 to 300 ms, with a resultant error of 13.6%.

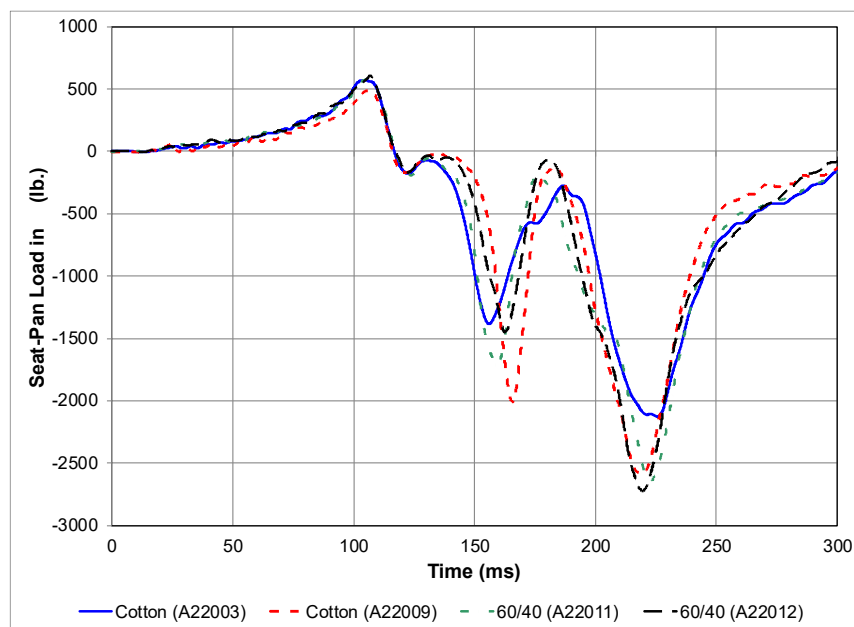


Figure 46: Seat-Pan Force in the X-Direction (60/40 and Cotton).

Table 15: Seat-Pan Loads (60/40 and Cotton).

Test	Clothing	Maximum Load (lb.)	Time (ms)	Minimum Load (lb.)	Time (ms)
A22003	100% Cotton	568	104	-2128	226
A22009	100% Cotton	483	105	-2580	219
A22011	60%/40% Poly	585	107	-2650	222
A22012	60%/40% Poly	602	107	-2725	220

Seat Belt Restraint Loads

The first peak load occurred when the ATD's pelvis had achieved full forward movement. All four initial peaks were achieved at similar times, but the two 60/40 tests did not reach the loads achieved in the two 100% cotton tests ([Figure 47](#)). During the second peak, the 60/40 values fell between the baseline values. The shape error was calculated between A22003 and A22012, between 0 to 300 ms, and the result was an 8.6% difference.

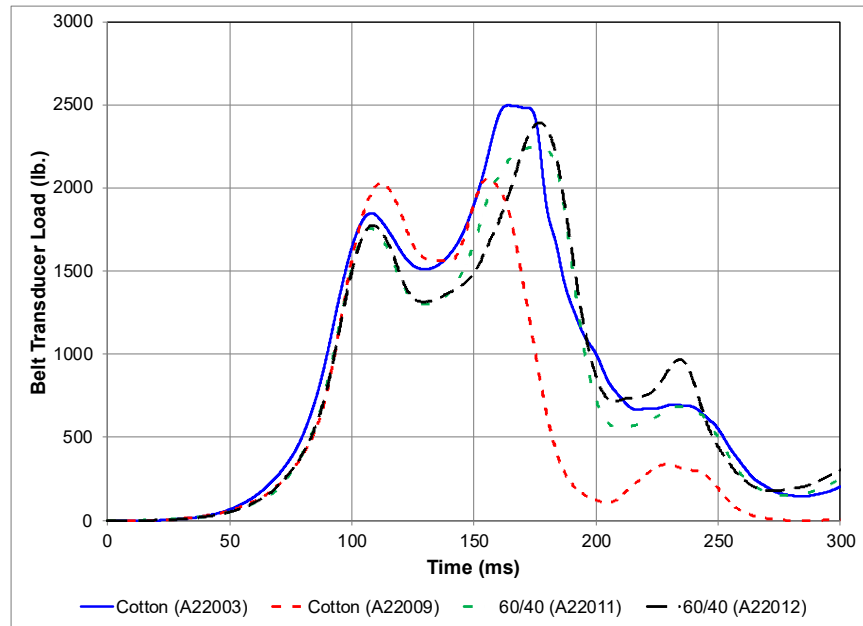


Figure 47: Belt-Transducer Loads (60/40 and Cotton).

Pelvis Angle

The two 60/40 pelvis angle curves fall between the two 100% clothing tests, for the full duration (*Figure 48*). The shape error was calculated between tests A22003 and A22012 and resulted in a 6.3% error.

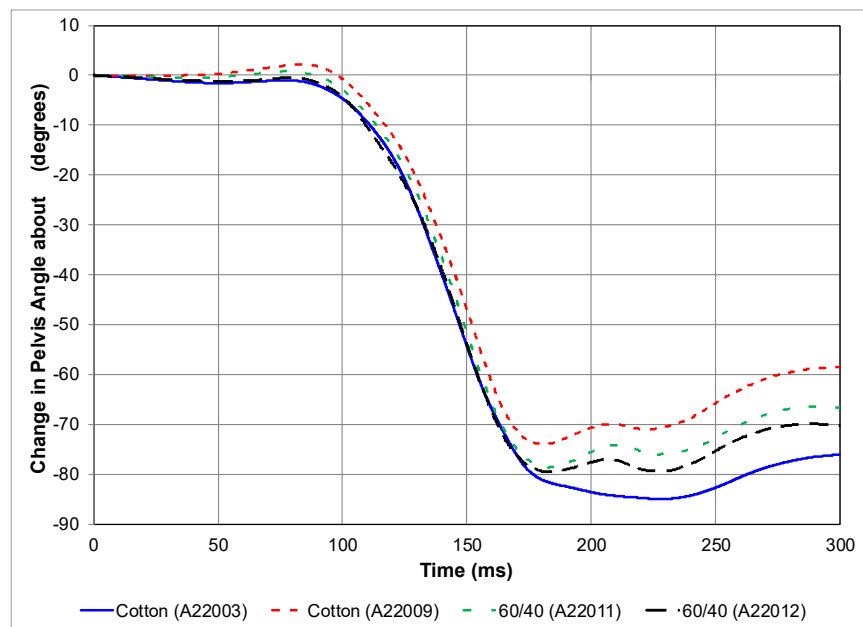


Figure 48: Change in Pelvis Angle about Y (60/40 and Cotton).

92% Polyester/8% Spandex vs. 100% cotton

Five tests were selected to compare 92% polyester/8% spandex (92/8) clothing and 100% cotton clothing. The tests from each group are: 92/8 (A21013, A21014 and A22014) and 100% cotton (A22003 and A22009). Only tests which had leg flail were included in the analysis

Head Path

The initial position, maximum head excursion in X, and minimum position in Z, with their respective times are listed in [Table 16](#). The maximum X-position measured in the 92/8 tests straddles the values in the 100% cotton tests. Whereas the minimum Z-position values from the 92/8 tests fall within the range of 100% cotton values.

Table 16: Head Path Values (92/8 and Cotton).

Test	Clothing	Footwear	X-Position at t=0 (in.)	Z-Position at t=0 (in.)	Max X-Position (in.)	Time (ms)	Min Z-Position (in.)	Time (ms)
A22003	100% Cotton	Mil Spec	5.8	45.2	44.5	175	6.0	222
A22009	100% Cotton	Mil Spec	6.1	45.8	44.6	174	7.5	218
A21013	92%/8% Poly	Bowling	5.6	45.1	44.7	173	6.9	214
A21014	92%/8% Poly	Bowling	6.0	45.7	45.3	173	7.4	212
A22014	92%/8% Poly	Bowling	5.6	44.8	43.9	173	6.4	209

The X-position versus Z-position head paths for the five tests are plotted in [Figure 49](#). The head path of X-position versus time is plotted in [Figure 50](#) and Z-position versus time is plotted in [Figure 51](#). The X-position versus time plot overlays until the maximum value is reached at ~180 ms. The Z-position versus time plots overlay for most of the test duration, diverging after about 225 ms. The shape error was calculated between A22003 and A22014 was 2.6% for X-position versus time and 2.4% for Z-position versus time.



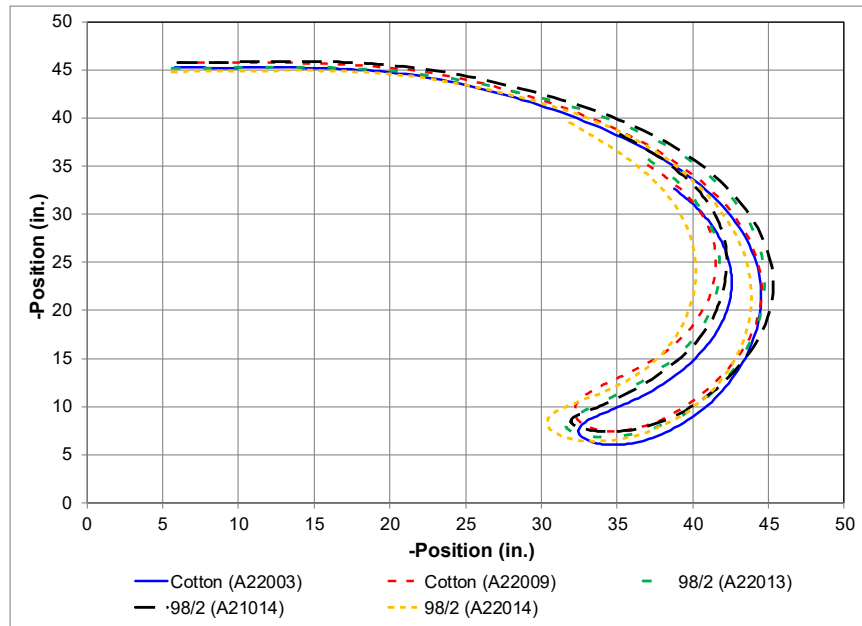


Figure 49: Head Path for 92/8 and Cotton: X-Position vs. Z-Position.

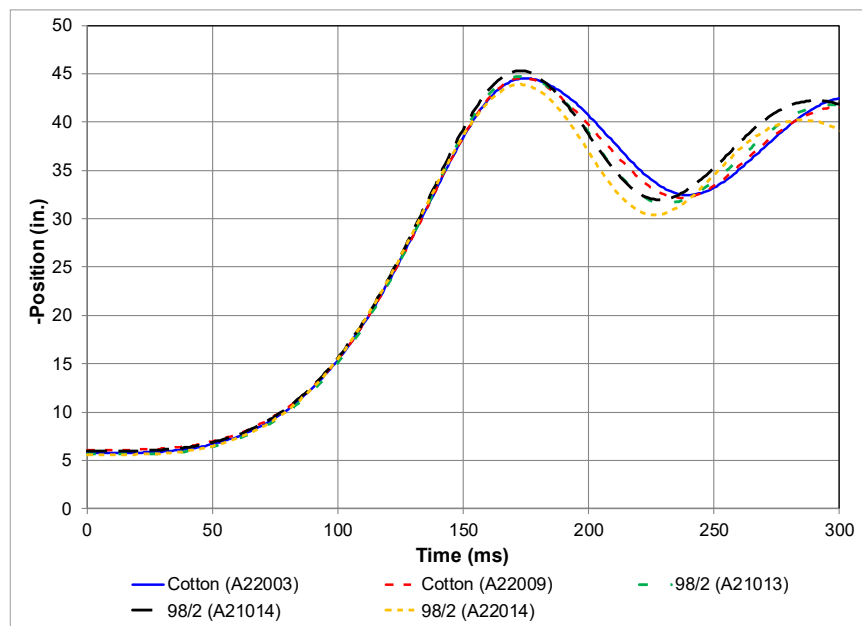


Figure 50: Head Path for 92/8 and Cotton: X-Position vs. Time.

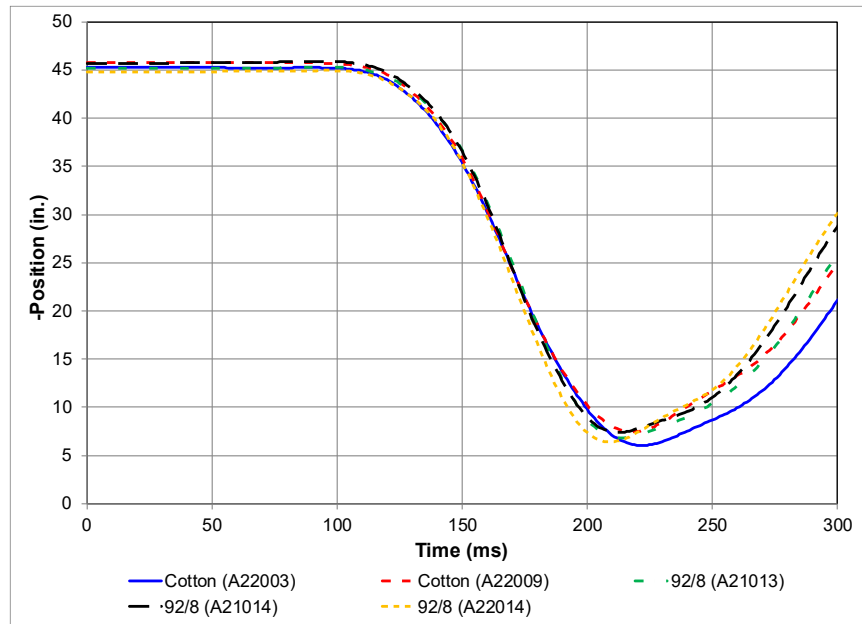


Figure 51: Head Path for 92/8 and Cotton: Z-Position vs. Time.

Seat-Pan Loads

The seat-pan load curves have a similar initial peak load at ~115 ms. From 115 ms to 200 ms, the shape of the three 92/8 curves diverge from the 100% cotton curves ([Figure 52](#)). The five curves reach their maximum negative peak within 20 ms of one another (207 to 226 ms) and follow the same trend from 200 ms until the end of the observed time of 300 ms. [Table 17](#) presents the peak positive and negative loads, with their respective times. The shape error was calculated between tests A22003 and A22014 was 24.6% difference.

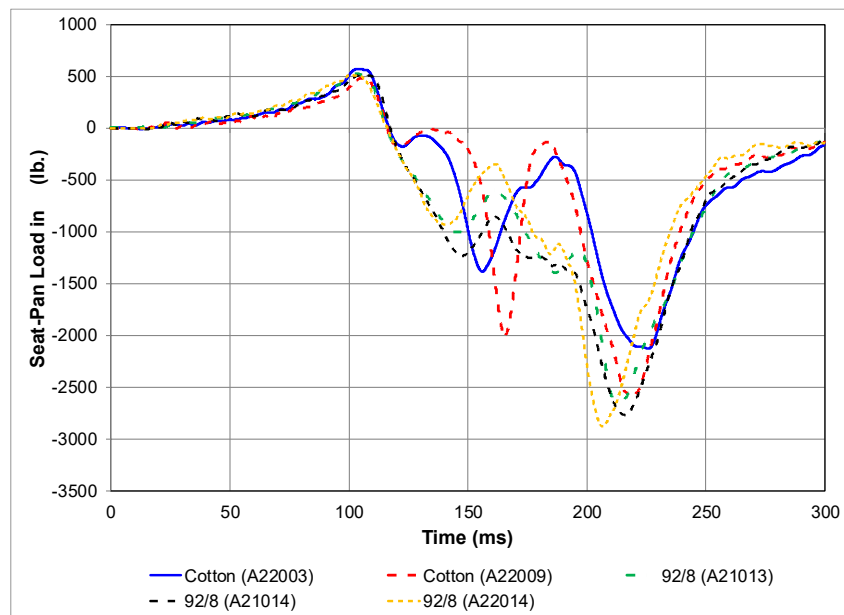


Figure 52: Seat-Pan Loads in the X-Direction (92/8 and Cotton).

Table 17: Seat-Pan Loads (92/8 and Cotton).

Test	Clothing	Maximum Load (lb.)	Time (ms)	Minimum Load (lb.)	Time (ms)
A22003	100% Cotton	568	104	-2128	226
A22009	100% Cotton	483	105	-2580	219
A21013	92%/8% Poly	523	103	-2654	213
A21014	92%/8% Poly	518	106	-2765	216
A22014	92%/8% Poly	515	101	-2878	207

Seat Belt Restraint Loads

The three 92/8 belt-transducer loads all had maximum peaks at or above the 100% cotton belt loads (*Figure 53*). The shape of the five curves is similar, with each showing a typical double peak profile. Tests A22003 and A22014 were selected to calculate the shape error, resulting in a difference of 6.5%.

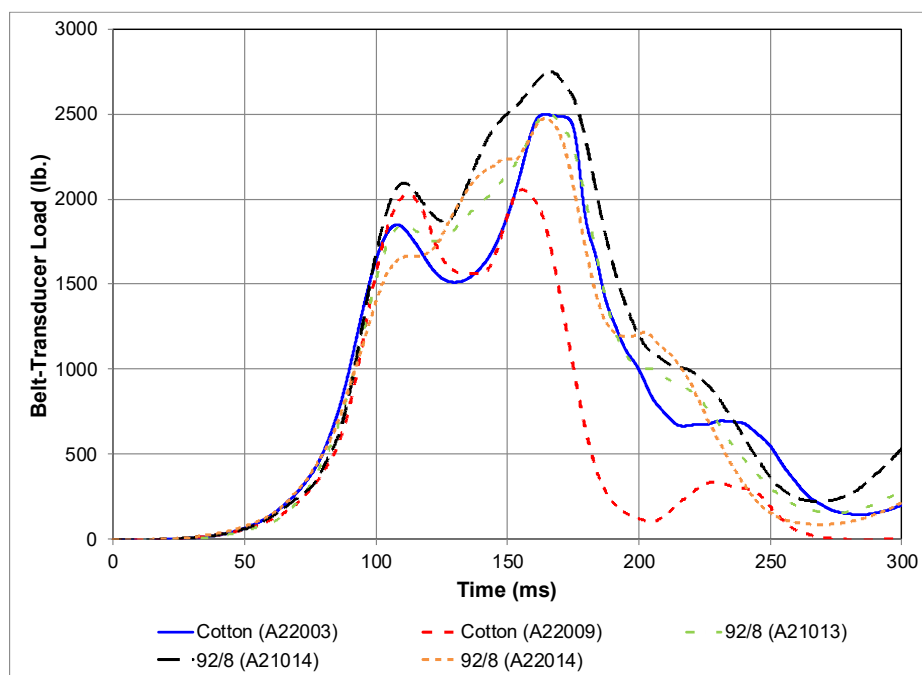


Figure 53: Seat Belt Loads (92/8 and Cotton).

Pelvis Angle

Figure 54 shows the change in pelvis angle for the three 92/8 and two 100% cotton tests. Two of the three 92/8 curves lie between the two cotton curves during the plateau (approximately 150 ms to 300 ms). Test A21014 did not reach the same angle as test A22009 until approximately 275 ms. Tests A22003 and A22014 were used to calculate the shape error of 10.5%.

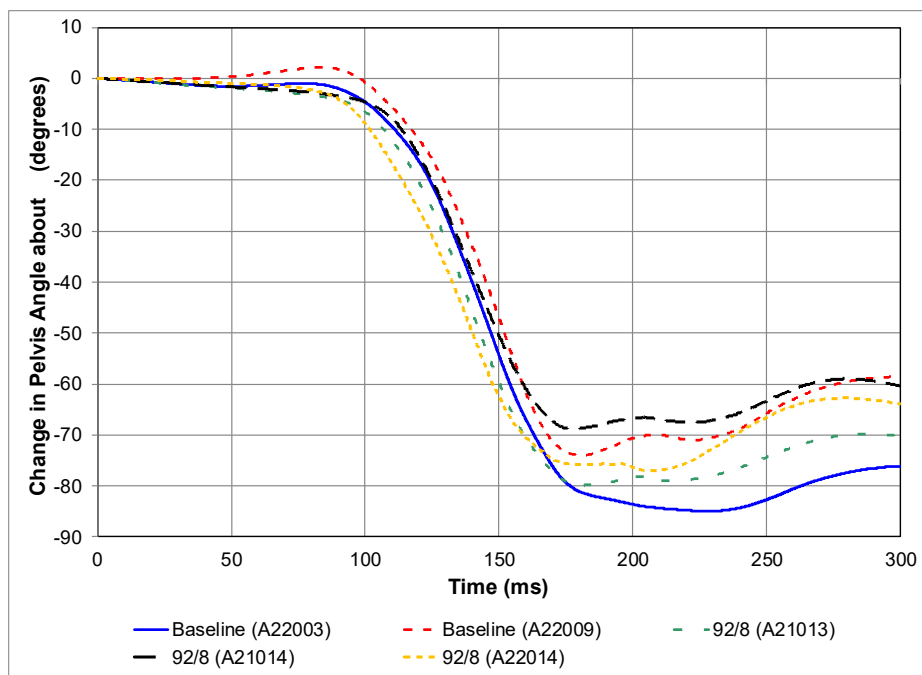


Figure 54: Change in Pelvis Angle about Y (92/8 and Cotton)

Summary - Effect of Clothing in Longitudinal Tests

Figure 55 presents a bar chart of the average head excursion for the three clothing combinations, with error bars representing the observed data range. The variance for 100% cotton was 0.1 in., 60/40 was 0.8 in., and 92/8 was 1.4 in. Using the same approach, as in the footwear summary, the head path range (X-direction) is assumed to be 1 in. for the 100% cotton clothing and is indicated with red horizontal lines representing the maximum and minimum values. The assumed 100% cotton range encompasses the full range of the 60/40 results and approximately 70% of the 92/8 results.

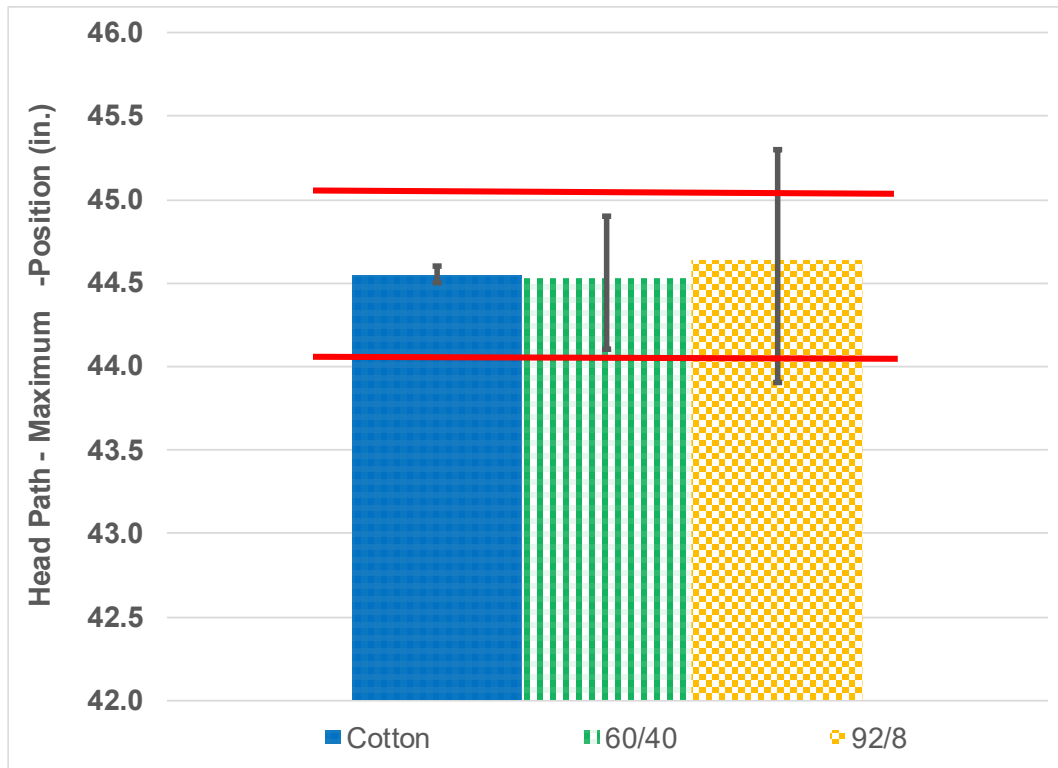


Figure 55: Clothing Head Path Bar Chart.

The comparisons of the seat belt restraint data and the pelvis angle data showed only minor differences with different clothing, since most data curves from the alternative clothing lie within the data curves of the 100% cotton clothing. The biggest difference in results was seen in the seat-pan loads. All the maximum loads achieved with the 60/40 and 92/8 were higher than the 100% cotton clothing. The use of the alternate clothing resulted in higher seat-pan loads. Based on this data, clothing had a minor effect on the occupant response in a Part 25 longitudinal test.

Effect of an Apron in Longitudinal Tests

A leather apron was used in three longitudinal tests: A22007, A22008, and A22010. The only apron test that achieved leg flail was A22007. Therefore, the comparison was limited to test A22007 and the two baseline apparel tests (100% cotton clothing and mil spec, A22003 and A22009). The goal of the apron tests was to evaluate the change in pretest ATD positioning, pretest restraint angles, dynamic results, and damage mitigation. Head path was evaluated because it is the most critical kinematics metric for a longitudinal test and reflects the global influence of friction. The seat-pan and floor-pan loads were used to determine change of the ATD's interaction with these surfaces. The pelvis angle and the seat belt restraint loads were used to determine the effect of friction between the apron and the belt.

ATD Position and Pretest Restraint Angle

The coordinate-measuring machine (CMM) was used to record the pretest position of the ATD and the angle of the restraint across the ATD's pelvis. All three baseline and all three apron tests were compared for their initial positioning because the achieved initial position was independent of whether leg flail occurred during the dynamic test. [Table 18](#) provides the H-point's X- and Z-position. Without the apron, the X-position ranged from 4.4 in. to 5.3 in. on the left side and 3.7 in. to 4.3 in. on the right side. With the apron, the X-position ranged from 4.5 in. to 5.4 in. on the left side and 3.4 in. to 4.2 in. on the right side. The addition of the apron had no noticeable effect on the initial position of the ATD.

Table 18: H-Point Pretest Position Values.

Test	Apron	Left (in.)	Left (in.)	Right (in.)	Right (in.)
A22003	No	4.4	24.9	4.3	24.5
A22006	No	5.3	24.6	3.7	24.7
A22009	No	4.4	24.6	3.7	24.8
A22007	Yes	5.4	24.7	3.4	24.5
A22008	Yes	4.6	24.7	3.6	24.6
A22010	Yes	4.5	24.7	4.2	24.7

The lap belt angle was calculated using the pretest CMM measurements and applying the calculation method defined in SAE International AS8049D. [Table 19](#) provides the left and right-side belt angles for the six tests. The left side belt angles ranged from 40.8° to 40.9° for all six tests. Without the apron the right-side angles ranged from 42.7° to 42.9°; with the apron the range was 42.7° to 43.0°. The placement of the leather apron made no significant change in the pretest restraint angle.

Table 19: Pretest Belt Angles.

Test	Apron	Left Belt Angle (°)	Right Belt Angle(°)
A22003	No	40.8	42.7
A22006	No	40.9	42.9
A22009	No	40.9	42.9
A22007	Yes	40.9	43.0
A22008	Yes	40.8	42.7
A22010	Yes	40.8	42.7

Head Path

As stated earlier, only tests with leg flail are included in the dynamic data comparisons. The apron test had a head displacement of 37.1 in. in the X-direction and 40.9 in. in the Z-direction ([Figure 56](#) and [Figure 57](#)). With the apron installed, the head did not extend as far in the X-position,

shorter by approximately 1 in., and approximately 3 in. in the Z-direction compared to the baseline tests. The shape error was calculated between tests A22003 and A22008: X-position versus time (1.0% error) and Z-position versus time (3.2% error).

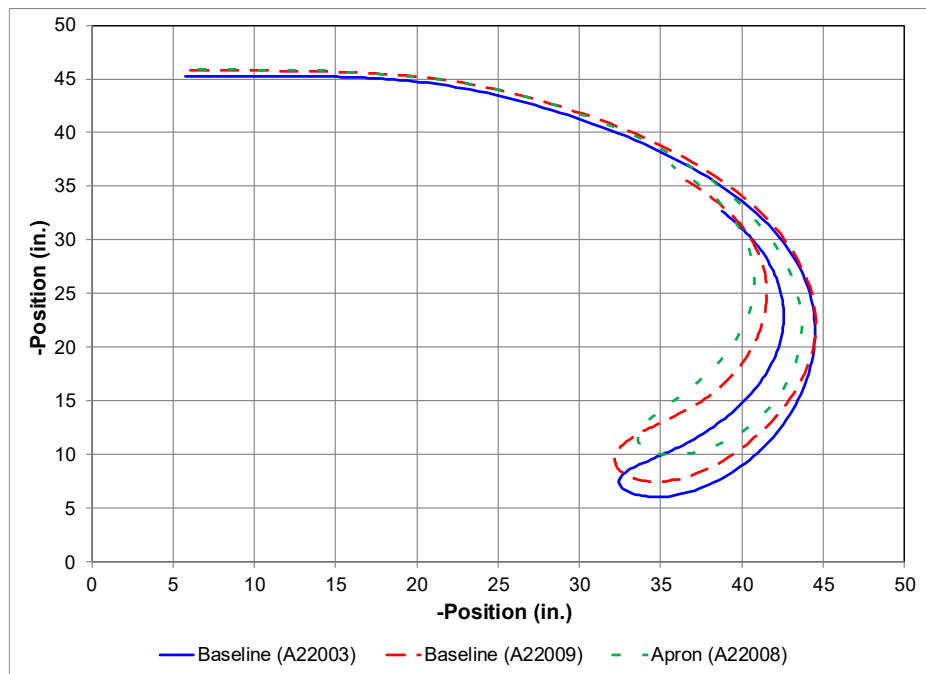


Figure 56: Head Path for Baseline and Apron.

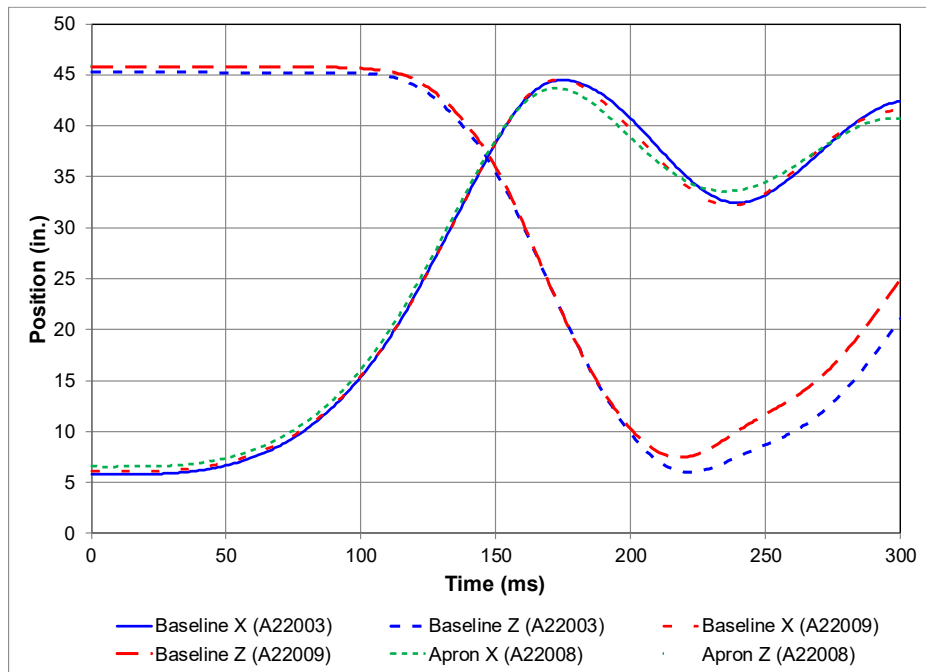


Figure 57: Head Path for Apron and Baseline: X & Z-Position vs. Time.

Seat-Pan Load

The seat-pan load in the X-direction for the two baseline tests and the apron test are plotted in [Figure 58](#). The three tests have similar shapes, although the magnitude and timing of peaks differ. All three curves achieve a positive peak at approximately 105 ms with a range of 483 lb. to 584 lb. Once the curves go negative around 125 ms, they diverge somewhat, with the apron test mostly falling in between the two non-apron tests. [Table 20](#) has the value for the maximum peaks and the minimum peaks with their respective time. Tests A22003 and A22008 were used to calculate the shape error, which resulted in 13.4%.

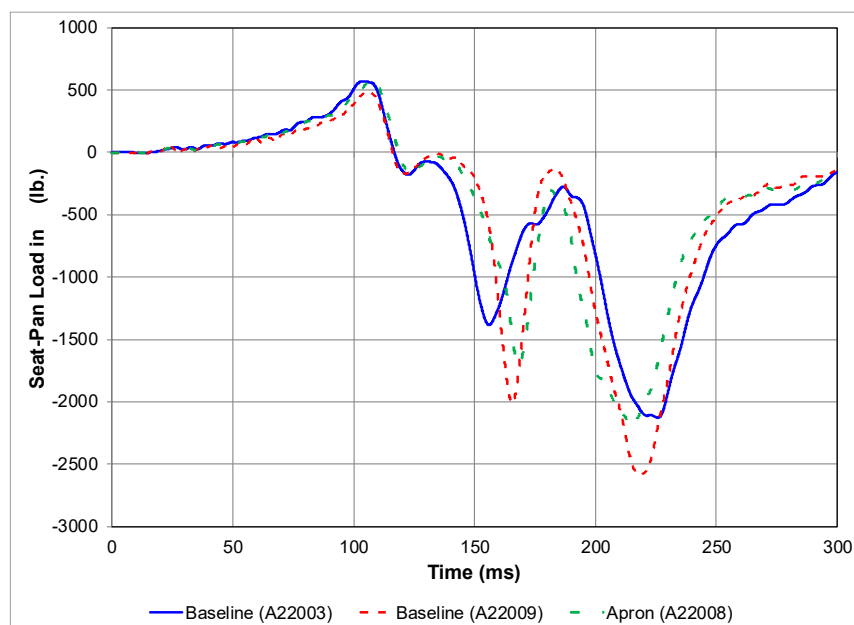


Figure 58: Seat-Pan Load in X-Direction for Apron and Baseline.

Table 20: Seat-Pan Loads (Apron and Baseline).

Test	Apron	Maximum Load (lb.)	Time (ms)	Minimum Load (lb.)	Time (ms)
A22003	No	568	104	-2128	226
A22009	No	483	105	-2580	219
A22008	Yes	575	108	-2195	215

Floor-Pan Load

The floor loads in the X-direction follow a similar shape up to 100 ms ([Figure 59](#)). The difference in loads at the first peak was approximately 40 lb. With the apron, the maximum load was achieved at 137 ms, approximately 30 ms before the foot came off the floor pan. [Figure 60](#) is the still images of the ATD's position at the maximum floor load and the last frame with the ATD's foot touching the floor. The shape error, calculated from 0 to 167 ms between tests A22003 and A22008, was 40.0%.

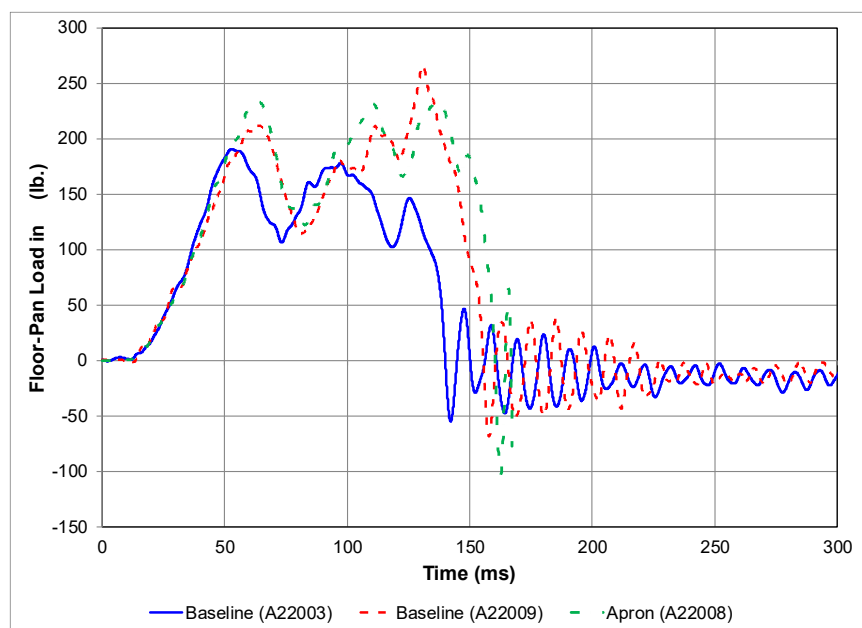


Figure 59: Floor Load in X-Direction for Apron and Baseline².



Figure 60: A22008 Picture of Peak Floor Load at 137 ms (Left) and Last Frame with Feet Touching Floor Pan at 158 ms (Right).

Seat Belt Restraint Loads

Figure 61 shows the belt-transducer loads for the three comparison tests. All three tests showed a typical double peak shape. Table 21 has the left belt anchor resultant load, right belt anchor resultant load, and the webbing-transducer loads from these tests. The apron test (A22008) had a similar initial peak as the first non-apron test (A22003). The second peak value for the apron test fell between the non-apron peaks, but the time at which the peaks occurred varied: 155 ms

² Test A22008 data was plotted from 0 to 167 ms due to a loose floor load-cell connector after this time.

(A22009), 164 ms (A22003), and 182 ms (A22008). The shape error was calculated between the curves for A22003 and A22008 and the result was 10.7%.

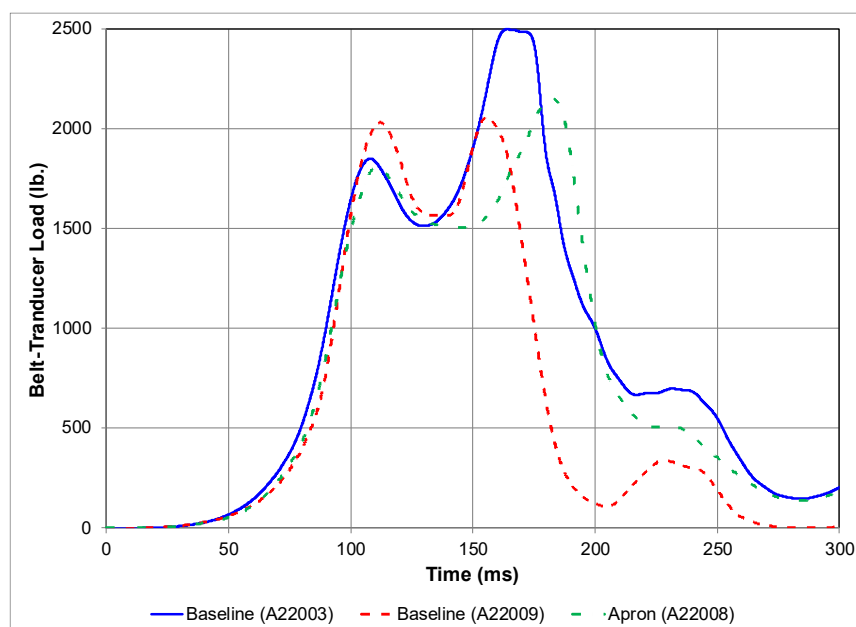


Figure 61: Belt-Transducer Load for Apron and Baseline.

Table 21: Peak Seat Belt Loads (Apron and Baseline).

Test	Apron	Left Belt Anchor Resultant Load (lb.)	Right Belt Anchor Resultant Load (lb.)	Webbing Transducer (lb.)
A22003	No	2392	2399	2496
A22009	No	2238	2070	2055
A22008	Yes	2594	2083	2149

Pelvis Angle

With the apron, the pelvis angle did not achieve the same maximum rotation as the baseline tests (*Figure 62*). The change in pelvis angle peaked at -69.1° with the apron, where -85.0° (A22003) and -74.0° (A22009) were achieved without the apron. The shape error was calculated using A22003 and A22008, and the result was a 22.5% difference.

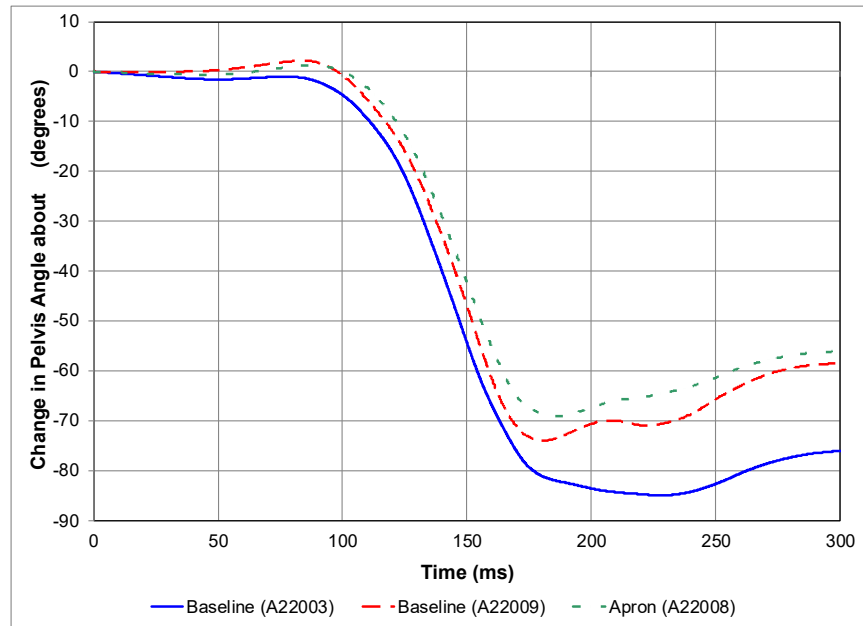


Figure 62: Change in Pelvis Angle about Y (Apron and Baseline).

Pelvis Damage

Damage caused by the belt buckle to the pelvis foam and rubber cover was observed after only seven longitudinal tests (*Figure 63*). The damage to the ATD pelvis after all 24 longitudinal tests is shown in *Figure 64*. *Figure 65* shows damage on both sides of the apron after the first apron test. The right side of the apron was damaged by the webbing and the left side was damaged by the buckle. By the end of all three apron tests, the cumulative wear and stress resulted in a roughly 1-inch hole developing in the leather, clearly visible in *Figure 66*. This hole highlights the significant material wear caused by repeated buckle impact throughout testing.



Figure 63: ATD Pelvis Damage from Belt Buckle after Seven Longitudinal Tests.



Figure 64: Damage to Pelvis at Completion of Testing.

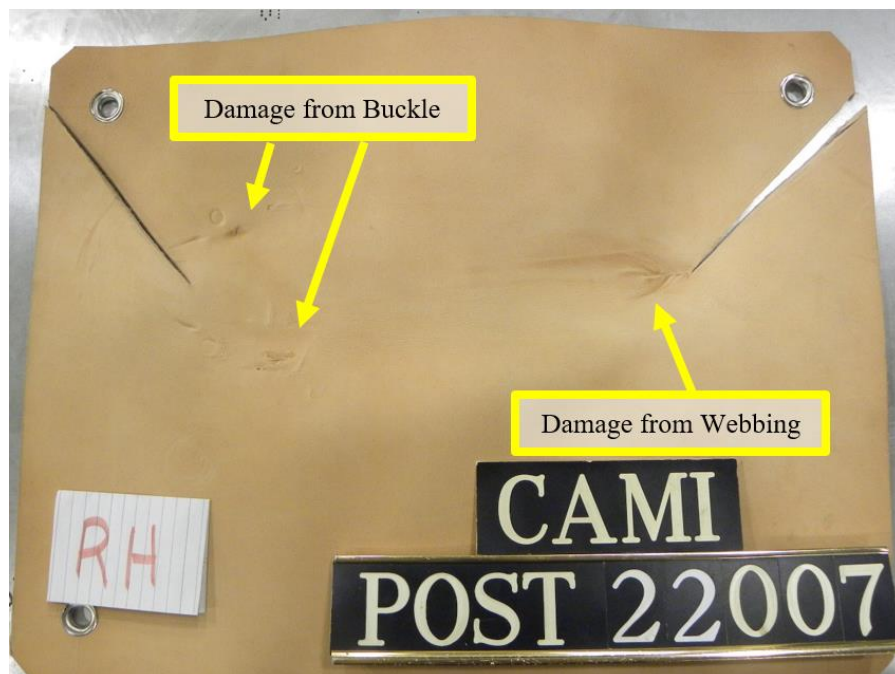


Figure 65: Leather Apron Damage After One Test.

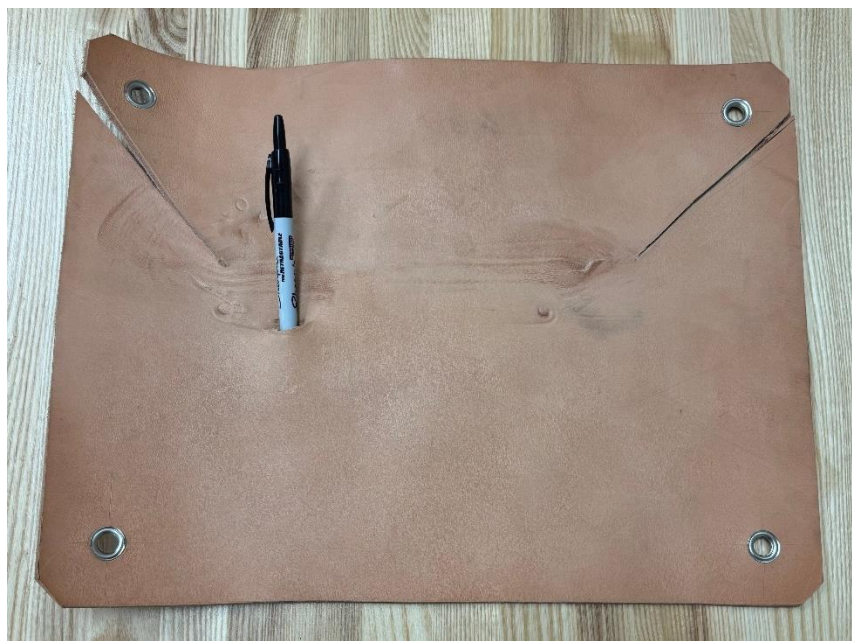


Figure 66: Leather Apron Damage at the Completion of testing. Permanent Marker for Position and Scale of Hole.

Summary - Effect of an Apron in Longitudinal Tests

The results of the testing showed that the addition of the apron was negligible in the initial ATD positioning, seat-pan loads, floor-pan loads, and belt loads. The ATD movement with the apron showed the largest differences in results with the head path 1 in. shorter in the X-direction and 3 in. higher in the Z-direction. The maximum pelvis angle achieved with the apron was 11 degrees lower than the results in the baseline apparel tests. The addition of the apron seemed to mitigate damage to the foam and rubber cover of the ATD pelvis. The legs flailed in one of the three tests with the apron, where the baseline apparel tests flailed in two of the three tests. Based on this data, it is unclear if the addition of an apron has an impact on leg flail. Additional data is required to evaluate the use of an apron in certification testing. A comprehensive analysis should include assessing various apron materials of varying thicknesses.

Limitations

The initial test matrix was designed to facilitate a sufficient number of tests to compare each combination of clothing, footwear, and aprons. However, limited leg flail incidents occurred in eight of the longitudinal tests, resulting in the exclusion of 33% of the tests from the comparison. Evaluations, such as the sneaker versus mil spec comparison (refer to Table 11), incorporated a mix of 60/40 and 100% cotton clothing to enable multiple footwear comparisons. A lower occurrence of limited flail scenarios would have allowed for a greater number of direct comparisons.

This test series was performed using a rigid seat, which does not accurately replicate the conditions of an actual seat. The data collected should not be extrapolated for use in real seat

testing conditions. Floor interface loads were not measured, and any deformation present in a real seat could alter the results. Head path and belt data are likely to remain valid, pan loading results are less reliable due to the inability to account for required seat deformation in seat certification tests.

All clothing tested met the criteria for form fitting, long sleeve shirt and full-length pants. Alternatives such as loose clothing, short sleeves, and shorts were deemed out of scope of this project. The durability and longevity of the clothing was not evaluated and cannot be determined based on the data gathered in this series of tests.

The floor pan used in this test series was the standard CAMI download fixture. For the longitudinal tests this may have minimized the effect of footwear friction. The use of a longer floor that would match an aircraft interior may have shown greater differences in the footwear.

A single apron that was 3/16 in. thick was used in testing. Aprons of different thickness, shape or pliability may affect the ATD kinematics differently than the apron tested. The apron evaluation was limited to determining the effect on test results. Determination of the reduction in damage, if any, of the pelvis was deemed out of scope.

Conclusion

The FAA Civil Aerospace Medical Institute undertook a project to evaluate the effect of ATD apparel during dynamic impact testing for longitudinal and vertical test conditions. This project supports FAA Policy and Standards Division's goal of identifying data variability attributable to the ATDs and apparel. While clothing and footwear requirements are defined in an industry standard (SAE AS8049D), this apparel can be difficult to obtain. Occupant response was evaluated for alternative footwear and clothing, as well as the use of a protective leather apron to reduce wear and tear on the ATD pelvis. Significant differences in seat-pan load and head path were seen between longitudinal tests with and without leg flail, supporting the AS8049D requirement for unrestricted leg flail to maximize seat loading. However, there was not a consistent effect on the probability of leg flail based on footwear. When both legs freely flailed, only minor differences in the head path and floor-pan load were seen between the four tested footwear (mil spec, boots, bowling shoe, and sneakers). For vertical testing, there was no difference in lumbar load between the hardest (boots) and softest (sneakers) soles.

The three clothing materials tested (100% cotton, 60% cotton/40% polyester, and 92% polyester/8% spandex), the head path data was similar, but the seat-pan loads were higher for the 60/40 and 92/8 clothes. The use of the alternate clothing could be considered a worse-case scenario since the measured seat-pan loads were higher. The results indicate that using alternative clothing and footwear still provide valid results for certification testing.

The addition of the apron in longitudinal testing seemed to mitigate pelvis damage without adversely affecting initial position. Additional testing is required to provide conclusive dynamic testing results that would allow for an apron to be used during certification testing.

References

- DeWeese R., Moorcroft D., & Taylor A. (2021). *Lumbar Load Variability in Dynamic Testing of Transport Category Aircraft Seat Cushions* (Office of Aerospace Medicine Report, DOT/FAA/AM21-09). Federal Aviation Administration.
https://www.faa.gov/sites/faa.gov/files/data_research/research/med_humanfacs/oamtechreports/202109.pdf
- Emergency Landing Dynamic Conditions. 14 C.F.R. §25.562. (2022).
<https://www.govinfo.gov/app/details/CFR-2022-title14-vol1/CFR-2022-title14-vol1-sec25-562>
- Gowdy, V., DeWeese, R., Beebe, M., Wade, B., Duncan, J., Kelly, R., Blaker, J. (1999). A lumbar spine modification to the Hybrid III ATD for aircraft seat tests. SAE Technical Paper 1999-01-1609 <https://doi.org/10.4271/1999-01-1609>
- Moorcroft (2007). Selection of Validation Metrics for Aviation Seat Models. Fifth Triennial International Aviation Fire & Cabin Safety Research Conference, Oct 30, 2007.
<https://www.fire.tc.faa.gov/2007conference/files/Crashworthiness/TuesPM/MoorcroftMetric/MoorcroftMetricPres.pdf>
- Moorcroft D, DeWeese R, & Taylor A. (2010). Improving Test Repeatability and Methods. The Sixth Triennial International Fire & Cabin Safety Research Conference, Oct 25-28, 2010.
https://www.fire.tc.faa.gov/2010Conference/files/Crash_Dynamics_III/MoorcroftLumbarLoad/MoorcroftLumbarLoadPres.pdf
- SAE International. (2020). Performance Standard for Seats in Civil Rotorcraft, Transport Aircraft, and General Aviation Aircraft, SAE Standard AS8049D, Revised November 2020, Issued July 1990, <https://doi.org/10.4271/AS8049D>.
- SAE International. (2021). Analytical Methods for Aircraft Seat Design and Evaluation, SAE Standard ARP5765B, Revised March 2021, Issued October 2012, <https://doi.org/10.4271/ARP5765B>.
- SAE International. (2022a). Instrumentation for Impact Test Part 1 - Electronic Instrumentation, SAE Standard J211/1_202208, Revised August 2022, Issued October 1970, https://doi.org/10.4271/J211/1_202208.
- SAE International, (2022b). Instrumentation for Impact Test—Part 2: Photographic Instrumentation, SAE Standard J211/2_202204, Reaffirmed April 2022, Issued October 1970, https://doi.org/10.4271/J211/2_202204.
- SAE International. (2024). Sign Convention for Vehicle Crash Testing, SAE Standard J1733_202411, Reaffirmed November 2024, Revised November 2018, Issued December 1994, https://doi.org/10.4271/J1733_202411.



Appendix A

The coefficient of friction for each shoe was based on the average of the calculated coefficient of friction from tests with three weights: 7.65, 13.18, and 26.93 lb.

Table 22: Mil Spec Coefficient of Friction Measurements and Calculation (Average=0.97).

Total Weight (lb.)	Measured Sliding Force (lb.)	Calculated Coefficient of Friction
8.86	9.5	1.07
14.39	12.5	0.87
28.14	27.0	0.96

Table 23: Boots Coefficient of Friction Measurements and Calculation (Average=1.00).

Total Weight (lb.)	Measured Sliding Force (lb.)	Calculated Coefficient of Friction
9.18	9.0	0.98
14.17	14.5	0.99
28.46	29.0	1.02

Table 24: Bowling Shoe Coefficient of Friction Measurements and Calculation (Average=0.62).

Total Weight (lb.)	Measured Sliding Force (lb.)	Calculated Coefficient of Friction
8.51	5.6	0.66
14.04	8.5	0.61
27.79	16.5	0.59

Table 25: Sneaker Coefficient of Friction Measurements and Calculation (Average=1.32).

Total Weight (lb.)	Measured Sliding Force (lb.)	Calculated Coefficient of Friction
8.42	11.0	1.31
13.95	18.0	1.29
27.70	38.0	1.37



Appendix B

Dataset and Contact Information

Title: Evaluation of Anthropomorphic Test Device Apparel for Aircraft Certification

Principal Investigator: Ian Hellstrom – ORCID: 0000-0002-3972-3981

Affiliation: U.S. Department of Transportation, Federal Aviation Administration, Civil Aerospace Medical Institute

Contact Information: Aerospace Medical Research Division, 6500 S. MacArthur Blvd, AAM-632, Oklahoma City, OK 73169, Ian.T.Hellstrom@faa.gov, 405-954-5767

https://www.faa.gov/about/office_org/headquarters_offices/avs/offices/aam/cami/

Funder: Federal Aviation Administration (faa.gov)

Grant/Contract(s): N/A

Persistent link: <https://doi.org/10.21949/1529686>

Recommended Citation: Hellstrom, I., Moorcroft, D., Carroll, W. (2025). Evaluation of Anthropomorphic Test Device Apparel for Aircraft Certification [datasets]. U.S. Department of Transportation, Federal Aviation Administration. <https://doi.org/10.21949/1529691>

Project Abstract

As part of a larger project aimed at gaining a better understanding of factors that affect the quality of test results using anthropomorphic test devices (ATDs), the Federal Aviation Administration (FAA) researched the effects of ATD apparel in dynamic tests. Current standards are limited to 100% cotton form fitting clothing and footwear with a 1.5-inch heel height and a combined weight of 2.5 pounds for the pair. For this project, three different types of clothing were tested: 60% cotton/40% polyester, 92% polyester/8% spandex and 100% cotton (the current standard). Additionally, four types of footwear were tested: bowling shoe, boots, sneaker, and a military specification shoe (standard). The FAA requires two certification tests to certify aircraft seating. The first test is a longitudinal impact with a minimum change in velocity of 44 ft/sec and peak acceleration of 16 g. The second test consists of a combined longitudinal-vertical impact with a minimum impact velocity of 35 ft/sec, peak acceleration of 14 g, and an impact angle of 30° off vertical. For this report, twenty-one longitudinal tests were run to measure the effects of clothing and footwear. Three additional longitudinal tests were conducted to evaluate the use of a protective barrier across the lap to mitigate damage to the ATD from the belt. Six vertical tests were conducted to evaluate the effect of the footwear in that test configuration. ATD response and seating system loads were analyzed to determine the effects of different combinations of clothing and footwear. Only minor differences were seen between the four different footwear for both longitudinal and vertical testing. The alternative clothing had little impact of peak head excursion but produced higher seat-pan loads. Thus, use of the alternate apparel could be considered a worse-case scenario. Only one of three apron tests achieved leg flail, therefore a definitive conclusion cannot be made on the impact an apron has on testing.

Project start date: 10-23-2020

Project end date: 07-31-2025

Data Description

This dataset contains test data of anthropomorphic test device pelvises mounted vertically in rigid fixtures on a high-rate load frame. These data are created by physical experiments. Sensors include a load cell and a linear variable differential transducer. Data also includes photos from still cameras. The tests were conducted in 2021-2022. No existing data were used for this test series.

It is anticipated that aircraft seat manufacturers and test laboratories will benefit from access to this data as they design and test real aircraft seats and restraints. This dataset will also provide a public record to support potential rulemaking.

Roles & Responsibilities

The FAA Aerospace Medical Research Division (see Contact Information) is responsible for generating the data and is responsible for managing the data initially. This division is responsible for managing the internal project management processes to ensure adherence to the published data management plan (DMP). This process requires management review and sign-off at project start and close-out.

This dataset is hosted by NHSTA in the biodynamics test database at:

<https://www.nhtsa.gov/research-data/research-testing-databases#/biomechanics>

Standards Used

The dataset complies with the NHTSA Test Reference Guide available at <https://www.nhtsa.gov/databases-and-software/entree-windows>. The data files collected are saved in common file formats, including ascii text, .xls, .jpg, .avi, and .mp4. The file formats can be opened using commonly available software such as text editors, picture viewers, and video viewers. .xls files can be opened with Microsoft Excel or freely available software, such as OpenRefine.

Access Policies

These data files are in the public domain and can be shared without restriction. The data files contain no sensitive information.

Sensitive Data Policies

The data files contain no sensitive information.

Sharing Policies

The data are in the public domain and may be re-used without restriction. Citation of the data is appreciated. Please use the following recommended citation: Hellstrom, I., Moorcroft, D., Carroll, W. (2024). Evaluation of Anthropomorphic Test Device Apparel for Aircraft Certification [datasets]. U.S. Department of Transportation, Federal Aviation Administration. <https://doi.org/10.21949/1529686>



Archiving and Preservation Plans

Crash Test Database (which includes Vehicle, Biomechanics, and Component databases) is stored in the Amazon Aurora PostgreSQL database. The database is hosted in the DOT managed Amazon Web Services (AWS) cloud environment. Automated full database backups are taken daily, leveraging AWS relational database service backups. The retention period for the backups is 14 days. The database is secure and only accessible to selected DOT users while only on the DOT network.

The dataset will be retained in perpetuity.

FAA staff will mint persistent Digital Object Identifiers (DOIs) for each dataset stored in the Biomechanics Test Database. These DOIs will be associated with dataset documentation as soon as they become available for use. The Digital Object Identifiers (DOIs) associated with this dataset include: <https://doi.org/10.21949/1529691>.

The assigned DOI resolves to the repository landing page for the “Evaluation of Anthropomorphic Test Device Apparel for Aircraft” dataset, so that users may locate associated metadata and supporting files.

The Biomechanics Test Database meets all the criteria outlined on the “Guidelines for Evaluating Repositories for Conformance with the DOT Public Access Plan” page: <https://ntl.bts.gov/ntl/public-access/guidelines-evaluating-repositories>.

Applicable Laws and Policies

This data management plan was created to meet the requirements enumerated in the U.S. Department of Transportation's 'Plan to Increase Public Access to the Results of Federally-Funded Scientific Research' Version 1.1 <https://doi.org/10.21949/1529686> and guidelines suggested by the DOT Public Access website <https://doi.org/10.21949/1529691>, in effect and current as of July, 31, 2025.

